ResearchGate

See discussions, stats, and author profiles for this publication at: https://www.researchgate.net/publication/331561629

Interactions between River Flow and Seepage Flow

Thesis · September 2009

CITATIONS
0

READS
128

1 author:

Upaka Rathnayake
Sri Lanka Institute of Information Technology
96 PUBLICATIONS **386** CITATIONS

SEE PROFILE

Some of the authors of this publication are also working on these related projects:

Energy forecasting View project

Impact of climate change to water resources in Sri Lanka View project

All content following this page was uploaded by Upaka Rathnayake on 17 March 2019.

The user has requested enhancement of the downloaded file.

Interactions between river flow and seepage flow

by
Upaka Sanjeewa Rathnayake

A thesis submitted in partial fulfillment of the requirements for the degree of Master of Engineering

Examination Committee: Professor Norihiro Izumi
Professor Yasuyuki Shimizu
Dr. Yasunori Watanabe

Master's Thesis No. EG-M…
Division of Field Engineering for Environment
Graduate School of Engineering, Hokkaido University
September 2009

ACKNOWLEDGEMENTS

First and foremost, the author would like to express his gratitude to Professor Norihiro Izumi, his supervisor at river and Watershed Engineering Laboratory, Hokkaido University, for Professor Izumi's technical guidance and his timely encouragement during this research. Professor Izumi was with extreme patience during the entire period of time, especially with my mistakes, he pointed out the mistake patiently and helped me to correct myself. I would not be able to pursue this far without his patience, insight, and plentiful advice. He has been a great teacher not only to me but also to every student in his career.

The author would also like to express his gratitude to those who have contributed significantly to this study, in particular to:

- The Examination Committee, Professor Yasuyuki Shimizu; at Hydraulic Research Laboratory, Hokkaido University and Dr. Yasunori Watanabe; at Coastal and Offshore Engineering Laboratory, Hokkaido University, for the highly valued comments;

- Dr. Adichai Pornprpmmin; a lecturer at Department of Water Resources Engineering, Kasetsart University, Thailand and a Post doctoral researcher at River and Watershed Engineering Laboratory, Hokkaido University to the kind and informative explanations through out the author's study;

- MEXT Scholarship by Government of Japan, for without it the author will not be pursuing this research;

- Dr. K.R.B. Herath, Senior Lecturer, Department of Civil Engineering, University of Peradeniya, Sri Lanka for his guidance and information about the graduate studies. Without his guidance the author will not be pursuing his graduate studies

- His mother and father for their continuing encouragement especially during difficult times encountered during the course of this research;

- His friend Atinkut Mezgebu Wubuneh, a doctoral degree candidate at River and Watershed Engineering Laboratory, Hokkaido University for reading the proofs, his friends and lab mates for their help and company

Finally, the author would like to acknowledge the support, love, and challenges offered to him by the most important person in his life; Shanika Mihirani, his wife.

ABSTRACT

Many previous studies have been carried on the interactions between river flow and the seepage flow in the environmental and biological point of view. Even though the interactions between river flow and seepage flow is recognized as an important process in rivers, previous literature hardly touches on the stability or the limitations for the interactions. Since these interactions are occurred frequently at least in mountainous regions, the river flow cannot be well treated as a lined cannel flow. Understanding the stability of these interactions among river flow and the seepage flow would be advantages for several research areas; including river environmental engineering, ecological and biological studies.

The subsurface layer below the river is known as the "hyporheic zone" and it can be defined as a saturated band of sediment that surrounds river flow and forms a linkage between the river and the aquifer. The zone facilitates to have bidirectional interactions as up-welling interactions and down-welling interactions. The origin of these interactions is due to the pressure and velocity differences between the two layers. The large velocity difference between the river flow layer and the seepage flow layer causes the instability of the flows. Due to this flow instability, a reciprocating flow motion is generated between the hyporheic layer and the above. In addition flow obstructions create an upstream high-pressure zone and a downstream low-pressure zone, resulting in hyporheic circulation under the object.

The stability of these hyporheic interactions is analyzed using the linear stability analysis technique. Linear stability analysis technique is used to understand the stability of the natural phenomenon by many researchers. Navier-Stokes equations and Brinkman-Forchheimer equations are used in order to formulate the river flow and seepage flow interactions respectively. The open channel flow in river is analyzed using the mixing length turbulent model and spectral collocation method incorporated with the Chebyshev polynomials are used to perform the numerical solution of the perturbed equations. Stability diagrams are discussed with several slopes of the layers against the dimensionless particle diameter and wave number. It has been understood that the range for the occurrence of instability region increases with the slope of the combined river and seepage layers. However it is important to recognize another instability region which occurs even in the range of small dimensionless particle diameter with relatively high wave numbers.

Several experiments are carried out, in order to understand the hyporheic interactions. Seepage layer is modeled using a Hele-Shaw which is a longitudinal parallel plate model. Methylene blue is used as the tracer to understand the hyporheic interactions and the experiment is conducted for two slopes as 0.1% and 0.2%. It can be concluded that the dimensionless dominant wave numbers have an effect on the combined channel slope and the Froude number of the river flow. In addition, it can be concluded that the residence time of hyporheic interactions are increased with the height of the river layer.

Rough comparison between the theoretical analysis and the experimental observations is carried out. It can be concluded that the same tendency in the theoretical analysis and the experimental observations from the comparison figures.

Key-Words: river flow, seepage flow, linear stability analysis, perturbations, growth rate contours, Hele-Shaw model, Froude number

TABLE OF CONTENTS

LIST OF TABLES

LIST OF FIGURES

CHAPTER

1

INTRODUCTION

1.1 BACKGROUND

1.1.1 General Introduction

Interactions between river flow and seepage flow are understood or recognized as an important process in rivers. The exchange is a fundamental process that affects the transport and fate of contaminants and other ecologically relevant substances in streams or rivers *[28]*. Several theoretical studies and field studies have emphasized the importance of hydrological interactions between the river flow and the seepage flow *[1], [3], [12], [16], [20], [21]-[24], [26], [28], [30], [35], [38], [41], [43], [45] and [46]*. Most of the authors have used the "hyporheic interactions" as the terminology for these river flow and seepage flow interactions. Also the zone just downwards from the river bed is called the hyporheic zone and according to the importance, this zone is defined using various definitions by worldwide researchers.

This hyporheic zone may be simply defined as an active eco-tone between the surface stream and groundwater, which facilitates to exchange water, nutrients, and organic matter occur in response to variations in discharge and bed topography *[2], [4], [6], [9], [26] and [31]*. Definition of the hyporheic zone is given with the biological interactions specifically by some researchers *[36] and [44]*, where as some others in chemical reactions *[29] and [42]*. It can be seen that the hyporheic zone and its interactions are very important to several types of research fields and more commonly the gathered research fields give one of the ecological balances of the nature.

The hyporheic interactions can be sub-divided in to two parts as vertical hyporheic interactions and lateral hyporheic interactions. The hyporheic zone bounds the stream channel and the hydrology is bidirectional due to the continuous mixing between the stream water and groundwater *[8]*. The hyporheic zone and the interactions can be seen from the Figure 1.1 and Figure 1.2 gives a 3-dimensional view of the hyporheic zone and its interactions.

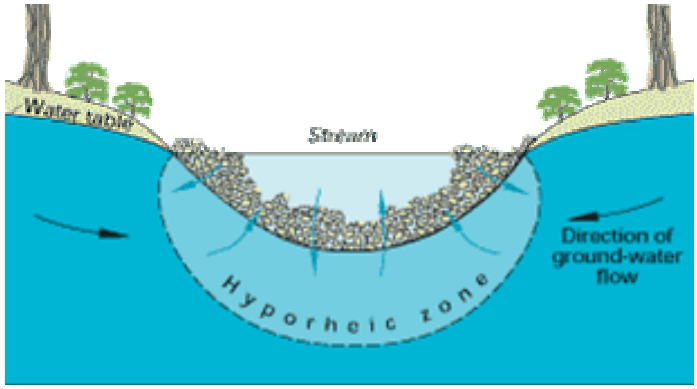

Figure 1.1 Hyporheic zone and its interactions
(Sustainability of Groundwater resources – circular 1186, by USGS, http://pubs.usgs.gov/circ/circ1186/html/gw_effect.html)

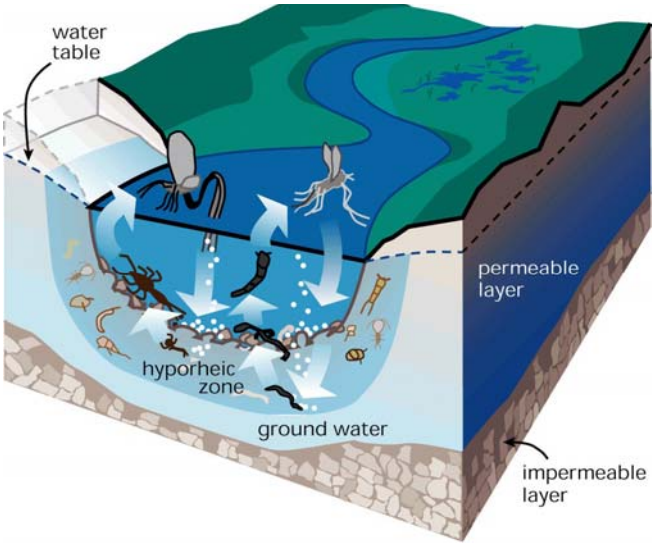

Figure 1.2 3-dimensional view of the hyporheic zone and its interactions
(Ecological Riverfront Design – Appendix A, 2001
www.americanrivers.org/assets/pdfs/appendix_a03bc.pdf*)*

Some typical parameters regarding the hyporheic zone and its interactions can be found from the literature. Some literature has cited that the hyporheic flow paths can be centimeters to tens of meters in length *[14]* and also it is typically considered by river ecologists to be only few centimeters to meters thick *[33]*.

1.1.2 Interactions in Hyporheic Zone

Some analysis shows that the hyporheic zone is facilitating to exchange at-least 10% of the river water flow *[40]*. Two interactions as "up-welling" and "down-welling" can be identified in the hyporheic interactions *[7]*. Up-welling subsurface water supplies river organisms with nutrients while down-welling river water provides dissolved oxygen, inorganic ions and organic matter to microbes and invertebrates in the hyporheic zone *[2], [4], [6], [21], [23], [28], [29], [35], [37], [41] and [43]*.

These up-welling and down-welling interactions influence the biogeochemistry of stream ecosystems by increasing solute residence times and more specifically solute contact with substrates in environments with spatial gradients in dissolved oxygen and pH *[18]*.

1.1.3 Occurrence of Hyporheic Interactions

Difference between river flow and seepage flow environments is one of the main reasons for the hyporheic interactions. Rivers typically have currents generating turbulences, short water residence times, variable discharges and physicochemical conditions, unidirectional transport of nutrients, sediments and biota, and a dynamic channel morphology. In contrast, alluvial groundwater environments are more stable, have longer water residence times, exhibit laminar flow, are permanently dark, and change little in sediment bed structure *[2]*.

In addition flow obstructions create an upstream high-pressure zone and a downstream low-pressure zone, resulting in hyporheic circulation under the object. In the same manner, bed forms, boulders, logs, or streambed irregularities created by biotic processes like salmon reeds generate down-welling fluxes in which river water is forced into the streambed and banks in regions of high pressure, and complimentary up-welling fluxes in which subsurface water is expelled into the river in regions of low pressure *[5] and [39]*. This process of advective pore water flow is known as pumping exchange *[10] and [11]*.

1.1.4 Factors Affecting Hyporheic Interactions

There are several factors that affect the hyporheic interactions according to the previous literature. Most of the factors deal with the hydraulic conductivity (the bed sediment diameter) and river morphology (the longitudinal slope of the river). Fine-scale granulometric features (size, shape, and composition of sediments) derive from catchment scale geological processes; determine most physical and chemical processes in the hyporheic zone *[3]*. Figure 1.3 shows a typical river in Hokkaido Island and it can be clearly observed that the features of bed materials which would lead the hyporheic interactions. In addition to some other researchers hyporheic exchange flow has been shown to be affected by stream morphology *[17] and [19]* , bathymetry *[10], [11] and [13]*, head gradient *[22] and [46]* and mean hydraulic conductivity *[2], [12] and [27]*.

Figure 1.3 Tottabetsu river, Hokkaido, Japan

1.2 AIMS OF THE RESEARCH

Literature shows that there is a great deal of research on the hyporheic interactions in the environmental and biological points of view, but few on the mechanism of interactions and the limitations for the interactions. Most research on riparian and hyporheic zones has focused on nutrient dynamics *[15]* as they are of major important for the protection of stream ecosystems and freshwater resources *[34]*. Also traditionally, most ecological research on groundwater and rivers has treated groundwater and rivers as distinct entities and has focused on within-system issues *[3]*. It is very important not to distinct the river flow and seepage flow which is beneath the river *[32]*. The structural heterogeneity that occurs on many different scales in river systems is obviously important for all surface–subsurface interactions, but little is known about the way in which sediment structure influences hyporheic exchange *[25]*.

- The first aim of this research is to understand the limitations or how the factors would affect the river flow and seepage flow interactions.
- The second aim of this research is to understand the river flow and seepage flow interactions by means of experiments using a Hele-Shaw model as the seepage layer.

1.3 SCOPE

With the available time and resources, following points have used in order to achieve the above mentioned aims of the research.

- Linear stability analysis has considered in the theoretical analysis and because of this linearity the theory would say the initiation of the interactions.
- Even though there are few other parameters which affect the river flow and seepage flow interactions, the author has considered its main parameters; particle diameter of the sediments and the longitudinal slope of the combined river flow and seepage flow.
- Flat bed condition has assumed for the river bed in order to ease the formulations and the analysis, even though the reality is not.
- Hele-Shaw model has used instead of the sediments in the seepage layer for the experiments, because of the difficulty of finding suitable sediments for seepage layer.

1.4 LAYOUT OF THE THESIS

Chapter 2 gives the detail literature review for the research work and it is sub-divided into few topics. Chapter 3 gives the theoretical work for the interactions between river flow and seepage flow. Linear stability analysis is shown in detail at the chapter. Chapter 4 gives the experimental work of the river flow and seepage flow interactions using a Hele-Shaw model. Rough comparison of theoretical and experimental work is found at the chapter 5 and the recommendations for further research are found at the last chapter, which is the chapter 6. The above mentioned chapters 3, 4 and 5 are with their results, conclusions and the cited references.

REFERENCES

[1] Barlow P.M., De Simone L.A. and Moench A.F., Aquifer response to stream stage and recharge variations. I. Analytic step-response function. *Journal of Hydrology*, 230, pp 192-210. 2000

[2] Boulton A.J., Findlay S., Marmonier P., Stanley E.H., and Valett H.M., The functional significance of the hyporheic zone in streams and rivers, *Journal of Annual Review of Ecological Systems*, 29, pp 59-81, 1998

[3] Brunke M. and Gonser T., The ecological significance of exchange processes between rivers and groundwater, *Journal of Freshwater Biology*, 37, pp 1–33, 1997

[4] Butturini A., Bernal S., Sabater S. and Sabater F., The influence of riparian-hyporheic zone on the hydrological responses in an intermittent stream, *Journal of Hydrology and Earth System Sciences,* 6(3), pp 515-525, 2002

[5] Cooper A.C., The effect of transported stream sediments on the survival of sockeye and pink salmon eggs and alevin, *Journal of International Pacific Salmon Fisheries Commission*, 18. 1965

[6] Daniele T. and Buffington M., Hyporheic exchange in gravel bed rivers with pool-riffle morphology; Laboratory experiments and three dimensional modeling, *Journal of Water Resources Research*, 43, 2007

[7] Dole-Olivier M-J, Marmonier P., Patch distribution of interstitial communities: prevailing factors, *Journal of Freshwater Biology*, 27, pp 177–191, 1992

[8] Duff J.H. and Triska F.J., Nitrogen biogeochemistry and surface-subsurface exchange in streams, *Streams and ground water*s, Jones J.B. and Mulholland P.J., (Editors), Academic Press, San Diego, USA, pp 197-220, 2000

[9] Edwards R.T., The hyporheic zone, *River Ecology and Management*: *Lessons from the Pacific coastal eco-region*, Naiman R.J. and Bilby R.E. (editors), pp 399–429, Springer, New York. 1998

[10] Elliott A.H., and Brooks N.H., Transfer of nonsorbing solutes to a streambed with bed forms: Theory, *Journal of Water resources research*, 33, pp 123-136, 1997

[11] Elliott A.H., and Brooks N.H., Transfer of nonsorbing solutes to a streambed with bed forms: Laboratory experiments, *Journal of Water resources research*, 33, pp 137-151, 1997

[12] Gilbert J., Danielopol D.L. and Stanford J.A. (editors), Groundwater Ecology, Academic Press, San Diego, 1994

[13] Harvey J.W. and Bencala K.E., The effect of streambed topography on surface-subsurface water exchange in mountain catchments, *Journal of Water Resources Research*, 29(1), pp 89-98, 1993

[14] Harvey J.W. and Wagner B.J., Quantifying hydrologic interactions between streams and their subsurface hyporheic zones, *Streams and ground waters*, Jones J.B. and Mulholland P.J., (Editors), Academic Press, San Diego, USA, pp 197-220, 2000

[15] Hill A.R., Stream chemistry and riparian zones, *Streams and ground waters*, Jones J.B. and Mulholland P.J. (Editors), Academic Press, San Diego, USA, pp 83-110, 2000

[16] Jones J.B., and Mulholland P.J. (Editors), *Streams and ground waters*, San Diego: Academic, pp 425, 2000

[17] Kasahara T. and Wondzell S.M., Geomorphic controls on hyporheic exchange flow in mountain streams, *Journal of Water resources research*, 39(1), 1005, 2003

[18] Kenneth E. B., Hyporheic zone hydrological processes, *Journal of Hydrological Processes*, 14, pp 2797–2798, 2000

[19] Maridet L., Philippe M., Wasson J.G., and Mathieu J., Spatial and temporal distribution of macro-invertebrates and trophic variables within the bed sediment of three streams differing by their morphology and riparian vegetation, *Journal of Archiv fur Hydrobiology*, 136, pp 41–64, 1996

[20] McDonnell J., McGlynn B.L., Kendall K., Shanley J. and Kendall C., The role of near-stream riparian zones in the hydrology of steep upland catchment, In: Hydrology, water resources and ecology in headwaters, *IAHS Publication* no. 248, pp 173-180, 1998

[21] Miglio E., Quarteroni A. and Saleri F., Coupling of free surface and groundwater flows, *Journal of Computational Fluids*, 32, pp 73–83, 2003

[22] Morrice J.A., Vallet H.M., Dahm C.N. and Campana M.E., Alluvial characteristics, groundwater-surface water exchange and hydrological retention in headwater streams, *Journal of Hydrological Process*, 11, pp 253-267, 1997

[23] Nakamura Y. and Stefan H.G., Effect of flow velocity on sediment oxygen demand: theory, *Journal of Hydraulic Engineering*, 120(5), pp 996–1016, 1994

[24] Packman A.I., Salehin M. and Zaramella M., Hyporheic exchange with gravel beds: basic hydrodynamic interactions and bed form-induced advective flows, *Journal of Hydraulic Engineering*, pp 647-656, 2004

[25] Packman A.I., Marion A., Zaramella N., Chen C., Gaillard J.F. and Keane D.T.., Development of layered sediment structure and its effects on pore water transport and hyporheic exchange, *Journal of Water, Air, and Soil Pollution*, 6, pp 433–442, 2006

[26] Runkel R.L., McKnight D.M. and Rajaram H., Modeling hyporheic zone processes, *Journal of Advances in Water Resources*, 26, pp 901–905, 2003

[27] Ryan R. J., and Packman A. I., Changes in streambed sediment characteristics and solute transport in the headwaters of Valley Creek, an urbanizing watershed, *Journal of Hydrology*, 323, pp 74-91, 2006

[28] Ryan R.J. and Boufadel M.C., Lateral and longitudinal variation of hyporheic exchange in a piedmont stream pool, *Journal of Environmental Science and Technology*, 41, pp 4221-4226, 2007

[29] Salehin M., Packman A.I., and Paradis M., Hyporheic exchange with heterogeneous streambeds: Laboratory experiments and modeling, *Journal of Water Resources Research*, 40, 2004

[30] Serrano S.E. and Workmann S.R., Modeling transient stream/aquifer interaction with non-linear Boussinesq equation and its analytical solution, *Journal of Hydrology*, 206, pp 245-255, 1998

[31] Smith J.W.N., Groundwater–surface water interactions in the hyporheic zone, *Science Report SC030155/SR1*, , Environment Agency (www.environment-agency.gov.uk), 2005

[32] Sophocleous M., Interactions between groundwater and surface water: the state of the science, *Journal of Hydrogeology*, 10, pp 52–67, 2002

[33] Stanford J.A., Ward J.V. and Ellis B.K., Ecology of the alluvial aquifers of the Flathead River, Montana, Gibert J., Danielopol D.L., and Stanford J.A. (editors), *Groundwater ecology*, Academic Press, San Diego, California, pp 367–390, 1994

[34] Standford J.A., Rivers in the landscape: Introduction to the special issue on riparian and ground water ecology, *Journal of Freshwater Biology*, 40, pp 402-406, 1998

[35] Steinberger N. and Hondzo M., Diffusional mass transfer at sediment–water interface, *Journal of Environmental Engineering*, 125(2), pp 192–199, 1999

[36] Storey R.G., Fulthorpe R.R., and Williams D.D., Perspectives and predictions on the microbial ecology of the hyporheic zone, *Journal of Freshwater Biology*, 41, pp 119– 130, 1999

[37] Strayer D.L., May S.E., Nielsen P., Wolheim W. and Hausam S., Oxygen, organic matter, and sediment granulometry as controls on hyporheic animal communities, *Journal of Archiv fur Hydrobiology*, 140 pp 131–144, 1997

[38] Taha A., Gresillon J.M. and Clothier B.E., Modeling the link between hill-slope water movement and stream flow: application to a small Mediterranean forested watershed, *Journal of Hydrology*, 203, pp 11-20, 1997

[39] Thibodeaux L.J. and Boyle J.D., Bed form-generated convective transport in bottom sediment, *Journal of Nature*, 325, pp 341– 343, 1987

[40] Triska F.J. , Kennedy V.C. , Avanzino R.J. , Zellweger G.W. , and Bencala K.E., Retention and transport of nutrients in a third-order stream in Northwestern California: hyporheic processes, *Journal of Ecology*, 70 (6), pp 1893-1905, 1989

[41] Trussell R.R. and Chang M., Review of flow through porous media as applied to head loss in water filters, *Journal of Environmental Engineering*, 125(11), pp 998–1006, 1999

[42] Valett H.M., Dahm C.N., Campana M.E., Morrice J.A., Baker M.A., and Fellows C.S., Hydrologic influences on groundwater-surface water eco-tones: Heterogeneity in nutrient composition and retention, *Journal of North American Benthology Society*, 16, pp 239– 247, 1997

[43] Vollmera S., Ramos F.S., Daebel H. and Kuhn G., Micro scale exchange processes between surface and subsurface water, *Journal of Hydrology*, 269, pp 3–10, 2002

[44] Williams D.D., and Hynes H.B.N., The occurrence of benthos deep in the substratum of a stream, *Journal of Freshwater Biology*, 4, pp 233–256, 1974

[45] Wondzell S.M. and Swanson F.J., Seasonal and storm dynamics of the hyporheic zone of a 4th-order mountain steam, I: hydrological processes, Journal of North American Benthological Society, 15, pp 3-19, 1996

[46] Wroblichy G.J., Campana M.E., Valett H.M. and Dahm C.N., Seasonal variation in surface-subsurface water exchange and lateral hyporheic area of two stream-aquifer systems, *Journal of Water Resource. Research*, 34, pp 317-328, 1998

Chapter 2

LITERATURE REVIEW

2.1 INTRODUCTION

A detail literature review is carried out to have an expanded view of the interactions between river flow and seepage flow. Aims of the literature review are to understand the necessary formulation and available past research which is related to the relevant topic. Sub titles 2.2 to 2.7 give the sub sections of the literature review.

2.2 NAVIER-STOKES EQUATIONS FOR RIVER FLOW

The motion of fluid substances, which can flow, was described by Claude Louis Navier and George Gabriel Stokes in 1822. Euler had already derived the equations for an ideal fluid in 1755 which did not include the effects of viscosity. However, to understand the physical phenomena of the real fluids the viscous terms should be included in the governing equations and Navier-Stokes equations solved the draw back. The Navier-Stokes equation can be written in dimensional manner as follows *[1], [2], [8] and [11]*.

$$\rho\left[\frac{\partial \tilde{U}_i}{\partial \tilde{t}}+\tilde{U}_j\frac{\partial \tilde{U}_i}{\partial \tilde{x}_j}\right]=-\frac{\partial \tilde{P}}{\partial \tilde{x}_i}+\tilde{\rho}\,\tilde{g}_i+\tilde{\mu}\frac{\partial^2 \tilde{U}_i}{\partial \tilde{x}_j\,\partial \tilde{x}_j} \tag{2.1}$$

where;

$$\tilde{U}_j\frac{\partial \tilde{U}_i}{\partial \tilde{x}_j}=\tilde{U}_1\frac{\partial \tilde{U}_1}{\partial \tilde{x}_1}+\tilde{U}_2\frac{\partial \tilde{U}_1}{\partial \tilde{x}_2}+\tilde{U}_3\frac{\partial \tilde{U}_1}{\partial \tilde{x}_3}+\tilde{U}_2\frac{\partial \tilde{U}_1}{\partial \tilde{x}_2}+\tilde{U}_2\frac{\partial \tilde{U}_2}{\partial \tilde{x}_2}+$$

$$U_2\frac{\partial U_3}{\partial x_2}+\tilde{U}_3\frac{\partial \tilde{U}_1}{\partial \tilde{x}_3}+\tilde{U}_3\frac{\partial \tilde{U}_2}{\partial \tilde{x}_3}+\tilde{U}_3\frac{\partial \tilde{U}_3}{\partial \tilde{x}_3} \tag{2.2}$$

$\tilde{U}_i, \tilde{P}, \tilde{\rho}, \tilde{\mu}, \tilde{g}_i$ and $\tilde{t}$ are the velocity of fluid particles, pressure, density of fluid, dynamic viscosity of fluid, gravitational acceleration and time respectively. The first term of the left hand side; $\frac{\partial \tilde{U}_i}{\partial \tilde{t}}$ of equation (2.1) is the time derivative inertial term. However, this term can be eliminated in some cases,

when the time is not so important. The second term of the left hand side; $\tilde{U}_j \frac{\partial \tilde{U}_i}{\partial \tilde{x}_j}$ of equation (2.1) shows the effect of time independent acceleration of a fluid with respect to space and it is the convection term. The first term of the right hand side; $\frac{\partial \tilde{P}}{\partial \tilde{x}_i}$ is the pressure variation in the river flow layer, $\tilde{\rho}\tilde{g}_i$ is the gravitational force term where the driving force for the flow and the last important term of the right hand side; $\tilde{\mu}\frac{\partial^2 \tilde{U}_i}{\partial \tilde{x}_j \partial \tilde{x}_j}$ is the viscous term.

2.3 BRINKMAN FORCHHEIMER EQUATIONS FOR SEEPAGE FLOW

The observations of Henry Darcy on the public water supply at Dijon and experiments on steady state unidirectional flow suggested Darcy's law, which in its refined modern form can be expressed as follows,

$$\frac{\partial \tilde{p}}{\partial \tilde{x}} = -\frac{\tilde{\mu}\tilde{v}_i}{\tilde{K}} \tag{2.3}$$

where $\partial \tilde{p} / \partial \tilde{x}$ is the pressure gradient, $\tilde{v}_i$ is the filtration velocity, $\tilde{\mu}$ is the fluid viscosity and $\tilde{K}$ is the permeability. The filtration velocity, $\tilde{v}_i$ (velocity averaged over the medium) is related to the intrinsic velocity, $\tilde{V}_i$ (velocity averaged over the pore space) by, $\tilde{v}_i = \lambda \tilde{V}_i$ where λ is the porosity. The permeability $\tilde{K}$ depends on the pore size or the particle diameter, $\tilde{d}_p$ and also on the detailed geometry. A useful estimate is given by the Carman-Kozeny relationship, derived for a packed bed of uniform spherical particles, namely

$$\tilde{K} = \frac{\tilde{d}_p^{\,2} \lambda^3}{180(1-\lambda)^2} \tag{2.4}$$

Darcy's law means that the drag is linearly proportional to the velocity. This holds for small velocities (namely when the Reynolds number based on the pore scale, is less than unity). However this law breaks down for larger velocities. Dupuit-1863 and Forchheimer-1901 found empirically, for larger

velocities, that the drag is a quadratic function of the velocity, and a detailed historical account has been given by Lage-1998, and what is commonly called the Forchheimer equation *[10]*.

A modern refinement of the Brinkman Forchheimer equation is given by the equation (2.5).

$$\frac{1}{\rho}\left(\frac{1}{\lambda}\frac{\partial \tilde{v}_i}{\partial \tilde{t}}+\frac{1}{\lambda^2}\left(\tilde{v}_i.\nabla \tilde{v}_i\right)\right)=-\nabla \tilde{p}+\tilde{\mu}_e\nabla^2\tilde{v}_i-\frac{\tilde{\mu}}{\tilde{K}}\tilde{v}_i-\frac{c_F\tilde{\rho}}{\sqrt{\tilde{K}}}\tilde{v}_i\left|\tilde{v}_i\right| \tag{2.5}$$

where $\tilde{\rho},\tilde{v}_i,\left|\tilde{v}_i\right|,\tilde{\mu}_e$ and c_F are the density of the incompressible fluid, Darcy's velocity, magnitude of the Darcy's velocity, effective viscosity and dimensionless Forchheimer coefficient respectively.

The first term of the left hand side; $\frac{1}{\lambda}\frac{\partial \tilde{v}_i}{\partial \tilde{t}}$ of equation (2.5) is the local time derivative inertial term and this has derived on the assumption that a spatial averaging process commutes with a derivative with respect to time and this breaks down when the porous medium has a macroscopic structure *[7]*. However it is essential to retain the time derivative term when modeling certain convective instability problems *[15] and [16]*.

The second term of the left hand side; $\frac{1}{\lambda^2}\left(\tilde{v}_i.\nabla \tilde{v}_i\right)$ of equation (2.5) is the advective inertia term which is encountered the inertial effects. The second term of the right hand side; $\tilde{\mu}_e\nabla^2\tilde{v}_i$ of equation (2.5) is the Brinkman viscous term and has a significant effect only in thin layers. However it is important to note that the Brinkman equation cannot be rigorously justified, except when the porosity is close to unity. The effective viscosity is found from the equation (2.6) *[10]*.

$$\tilde{\mu}_e=\tilde{\mu}/\lambda \tag{2.6}$$

$\nabla \tilde{p}$ is the pressure variation in the seepage layer, $\frac{\tilde{\mu}}{\tilde{K}}\tilde{v}_i$ is the Darcy's term for the flow through a porous media which is a dissipative force and the last term of the right hand side; $\frac{c_F\tilde{\rho}}{\sqrt{\tilde{K}}}\tilde{v}_i\left|\tilde{v}_i\right|$ of the equation (2.5) is the Dupuit Forchheimer (form drag) term and recommended by Joseph et al *[7]*. Initially c_F is assumed to be a universal constant but Ergun-1952 has imperially obtained the following formula for the spherical sediment.

$$c_F=\frac{1.75}{\sqrt{150}\lambda^{3/2}} \tag{2.7}$$

2.4 LINEAR STABILITY ANALYSIS

Linear stability analysis technique is widely used technique to understand the stability of a process at the initiation of the process. Since the analysis deals with the linear terms, this can only be used at the initiation of the processes. Stability analysis can simply be understood using the following example which is described in Figure 2.1.

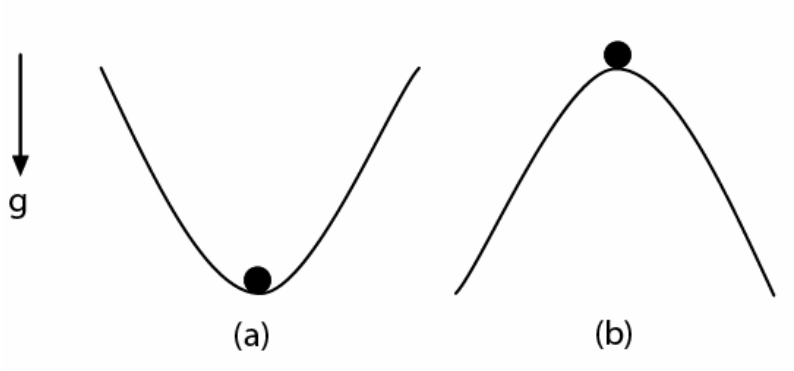

Figure 2.1 Stability of a sphere

The black colored ball is in equilibrium at both (a) and (b) stages but both are different each other. When a small horizontal perturbation applies for the sphere in both cases it can be observed out the following. At case (a) the sphere would move for a small distance inside the curve and come back to its initial position whereas at case (b) the sphere would move and not come to its initial position. Case (a) is at the "stable state" whereas case (b) is at the "unstable state" *[1]*.

Landau has worked on this stability problems in detail and the stability technique has explained using the Landau equation by the use of spectral collocation method as follows *[8]*.

$$\frac{dA}{dt} = \lambda_0 A + \lambda_1 |A|^2 A \tag{2.8}$$

where A, λ_0 and λ_1 are the amplitude of small perturbation, linear growth rate and Landau constant respectively. At the equilibrium stage the value of A can be found as follows.

$$\frac{dA}{dt} \to 0$$

$$A = \sqrt{-\frac{\lambda_0}{\lambda_1}} \tag{2.9}$$

However in the linear stability analysis the amplitude of the perturbation can be assumed to be infinitesimally small $\{ A \ll 1 \}$ and the Landau equation can be modified as equation (2.10)

$$\frac{dA}{dt} = \lambda_0 A \tag{2.11}$$

When $\lambda_0 < 0$, amplitude of the perturbation is reached to zero or else the amplitude is vanished, $A \to 0$. This can be concluded as the stable condition of the process. When $\lambda_0 > 0$ the amplitude of the perturbation reached to infinity, $A \to \infty$. This can be concluded as the unstable condition of the process. These two stages are shown in the Figure 2.2 in detail.

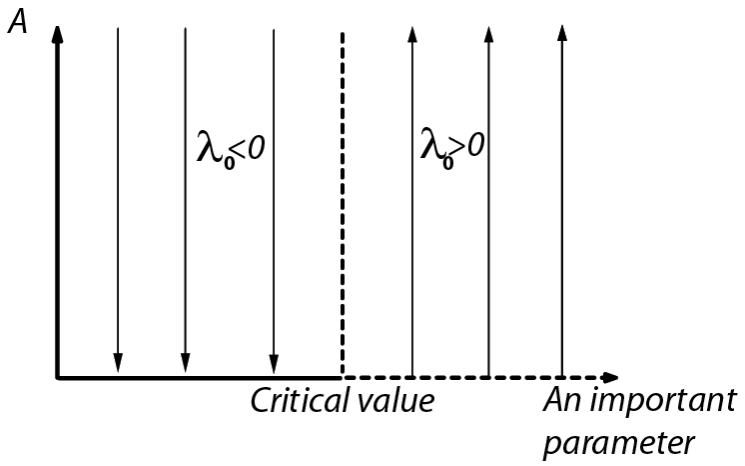

Figure 2.2 Stable and unstable conditions

2.5 CHEBYSHEV POLYNOMIALS

Chebyshev polynomials are a sequence of orthogonal polynomials *[4]* which are related to de Moivre's formula which is shown in equation (2.12) and which are easily defined recursively. Any complex number x and any integer n hold the following.

$$\left(\cos(x) + i\sin(x)\right)^n = \cos(nx) + i\sin(nx) \tag{2.12}$$

There are two kinds of Chebyshev polynomials and usually the first kind is denoted by T_n and the second kind is denoted by U_n. Chebyshev polynomials are important in approximation theory because the roots of the Chebyshev polynomials of the first kind, which are also called Chebyshev nodes, are used as nodes in polynomial interpolation. The resulting interpolation polynomial minimizes the problem of Runge's phenomenon and provides an approximation that is close to the polynomial of best approximation to a continuous function under the maximum norm.

The first kind of Chebyshev polynomials are defined by the recurrence relation as follows.

$T_0(x) = 1$

$T_1(x) = x$

$T_{n+1}(x) = 2xT_n(x) - T_{n-1}(x)$

One example for generating function can be shown in the equation (2.13)

$$\sum_{n=0}^{\infty} T_n(x)t^n = \frac{1-tx}{1-2tx+t^2} \tag{2.13}$$

The second kind of Chebyshev polynomials are defined by the recurrence relation as follows.

$$U_0(x) = 1$$
$$U_1(x) = 2x$$
$$U_{n+1}(x) = 2xU_n(x) - U_{n-1}(x)$$

One example for generating function can be shown in the equation (2.14)

$$\sum_{n=0}^{\infty} U_n(x)t^n = \frac{1}{1-2tx+t^2} \tag{2.14}$$

Also these two kinds can be expanded using the trigonometric functions.

2.6 SPECTRAL COLLOCATION METHOD

Spectral collocation methods are a class of techniques used to numerically solve certain partial differential equations, often involving the use of the Fast Fourier Transform. The method can be used to write the solution as a Fourier series and by substituting this series into the partial differential equations, a system of ordinary differential equations. It means that a linear combination is approximated in the spectral collocation method *[6]*.

2.7 HELE-SHAW MODEL

Hele-Shaw in 1897, has proposed a parallel plate model forming a narrow channel and this viscous flow model was first used by Hele-Shaw to study the nature of flow around obstructions of various shapes *[14]*. In 1936 it was used for the first time in groundwater investigations by Dachler *[3]*. However later it is widely used to analyze the groundwater flow in a 2-dimensional cross section of an aquifer *[3], [5], [9], [12] and [13]*. A parabolic velocity distribution for a laminar flow is usually assumed in between the plates and the flow is defined by the Navier-Stokes equations. Permeability of a Hele-Shaw can be usually found from the equation (2.15) which is a function of the gap width, but this is little bit deviated to the equation (2.16), when the porous medium plays an important role to the analysis *[5]*.

$$\tilde{K} = \frac{b^2}{12} \tag{2.15}$$

$$\tilde{K} = \frac{b^3}{12d} \tag{2.16}$$

where b and d are the gap or space between two plates and the thickness of the plate of the Hele-Shaw model.

REFERENCES

[1] Acheson D.J., *Elementary fluid dynamics*, 1st edition, Oxford University press, ISBN 0-19-859679-0 Chapter 6, pp 201-217, 1990

[2] Cengel Y.A. and Cimbala J.M., *Fluid mechanics: Fundamentals and applications*, McGraw Hill Companies, ISBN 0-07-111566-8, Chapter 10 pp 471-560, 2006

[3] Columbus N., The design and construction of Hele-Shaw models, *Groundwater*, 4, pp 16-22, 1966

[4] Grewal B.S., Higher Engineering Mathematics, 35th edition, Khanna publishers, ISBN 81-7409-084-3, Chapter 14, pp 439, 2000

[5] Hartline B.K., An experiment to verify the permeability of Hele-Shaw cells, *Journal of Geophysical research letters*, 5, pp 225-227, 1978

[6] Hussaini M.Y.and Zang T.A., Spectral methods in fluid dynamics, Annual review of Fluid Mechanics, 19, pp 339-367, 1987

[7] Joseph D.D., Nield D.A. and Papanicolaou G., Nonlinear equation governing flow in a saturated porous medium, *Journal of water resources research*, 18, pp 1049-1052, 1982

[8] Landau L.D. and Lifshitz E.M., *Fluid mechanics*, 2nd edition, Pergamon press, ISBN 0-08-033933-6, Chapter 2, pp 44-94, 1987

[9] Marino M.A., Hele-Shaw model study of the growth and decay of groundwater ridges, *Journal of geophysical research*, 72(4), pp 1195-1205, 1957

[10] Nield D.A., Modeling fluid flow in saturated porous media and at interfaces, *Transport phenomena in porous media II,* Ingham D.B. and Pop I. (editors), Pergamon publishers, ISBN 0080439659, Chapter 1, pp 1-19, 2002

[11] Schlichting H., Boundary layer theory, (translated by Kestin J.), 7th edition, McGraw Hill Companies, ISBN 0-07-055334-3, Chapter 3, pp 47-69, 1979

[12] Todd D.K., Unsteady flow in porous media by means of a Hele-Shaw viscous fluid model, *Journal of American geophysical union*, 35, pp 905-915, 1954

[13] Todd D.K., Laboratory research with groundwater models, *Proceedings of ASCE*, pp 199-206, 1955

[14] Todd D.K., *Groundwater hydrology*, John Wiley and Sons, New York, pp 336, 1959

[15] Vadasz P., Free convection in rotating porous media, *Transport phenomena in porous media*, Ingham D.B. and Pop I. (editors), Pergamon, Oxford, pp 285-312, 1998

[16] Vadasz P., Flow in rotating porous media, *Fluid transport in porous media*, Plessis P. (editor), Chapter 4, Computational mechanics publications, Southampton, 1999

Chapter

3

LINEAR STABILITY ANALYSIS OF THE INTERACTIONS BETWEEN RIVER FLOW AND SEEPAGE FLOW

3.1 INTRODUCTION

A detailed linear stability analysis has been carried out and this chapter presents the essentials of the linear stability analysis. Figure 3.1 shows the conceptual model which is used to formulate the both river and the seepage flow. Constant and same slope; S is assumed for both layers with the constant discharge in the stream-wise direction. The depth of the seepage layer is assumed to be comparable with the flow depth in the river flow layer and both river flow height and the seepage flow height have been noted as $\tilde{H}$ and $\tilde{h}$ respectively. $\tilde{x}$ is considered as the stream-wise direction and the $\tilde{y}$ is considered the normal direction to the stream wise direction in dimensional manner. The flow is assumed to be in the normal flow condition and if this normal flow condition is stable, there is no water exchange between flows inside and outside of the permeable layer. Limitations for these interactions are found from the theoretical analysis and the flow of this chapter to show the results and conclusions of the theoretical analysis.

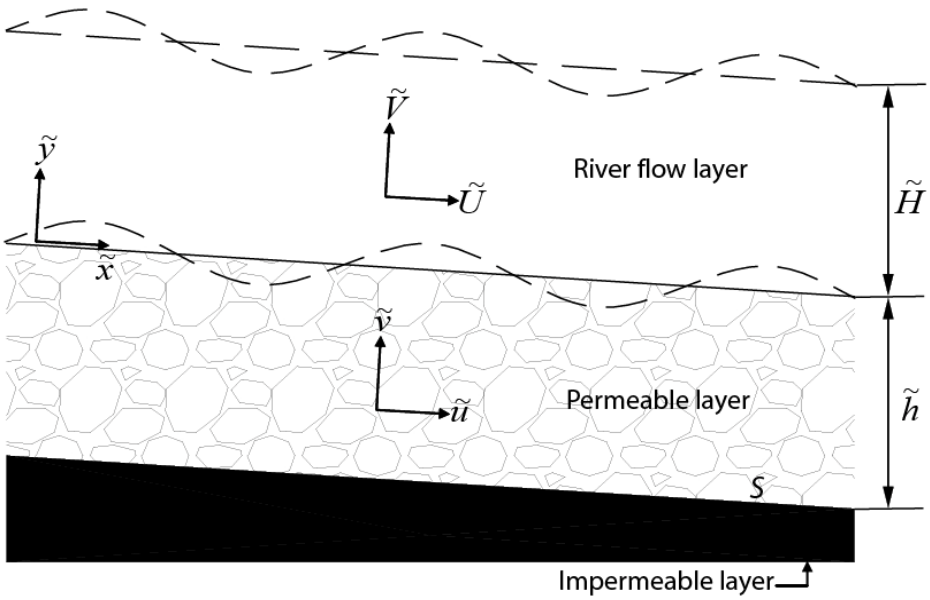

Figure 3.1 The conceptual diagram of the model

3.2 DIMENSIONAL MANNER OF THE RIVER FLOW GOVERNING EQUATIONS

Turbulent flow in river is formulated using the Navier-Stokes equations as follows.

Stream-wise direction - ($\tilde{x}$)

$$\frac{\partial \tilde{U}}{\partial \tilde{t}} + \tilde{U}\frac{\partial \tilde{U}}{\partial \tilde{x}} + \tilde{V}\frac{\partial \tilde{U}}{\partial \tilde{y}} = -\frac{1}{\tilde{\rho}}\frac{\partial \tilde{P}}{\partial \tilde{x}} + \frac{1}{\tilde{\rho}}\frac{\partial \tilde{T}_{xx}}{\partial \tilde{x}} + \frac{1}{\tilde{\rho}}\frac{\partial \tilde{T}_{xy}}{\partial \tilde{y}} + \tilde{g}_x \tag{3.1}$$

Normal to stream-wise direction - ($\tilde{y}$)

$$\frac{\partial \tilde{V}}{\partial \tilde{t}} + \tilde{U}\frac{\partial \tilde{V}}{\partial \tilde{x}} + \tilde{V}\frac{\partial \tilde{V}}{\partial \tilde{y}} = -\frac{1}{\tilde{\rho}}\frac{\partial \tilde{P}}{\partial \tilde{y}} + \frac{1}{\tilde{\rho}}\frac{\partial \tilde{T}_{xy}}{\partial \tilde{x}} + \frac{1}{\tilde{\rho}}\frac{\partial \tilde{T}_{yy}}{\partial \tilde{y}} + \tilde{g}_y \tag{3.2}$$

where;

$$\tilde{g}_x = \tilde{g}\sin\theta \tag{3.3}$$

$$\tilde{g}_x \simeq \tilde{g}\tan\theta \tag{3.4}$$

$$\tilde{g}_x \simeq \tilde{g}S \tag{3.5}$$

$$\tilde{g}_y = -\tilde{g}\cos\theta \tag{3.6}$$

$\theta \simeq 0$ (θ is the slope angle and assumed to be very small) (3.7)

$$\tilde{g}_y \simeq -\tilde{g}\cos 0 \tag{3.8}$$

$$\tilde{g}_y \simeq -\tilde{g} \tag{3.9}$$

Then the governing equations are re-written to the following (3.10) and (3.11) equations.

$$\frac{\partial \tilde{U}}{\partial \tilde{t}} + \tilde{U}\frac{\partial \tilde{U}}{\partial \tilde{x}} + \tilde{V}\frac{\partial \tilde{U}}{\partial \tilde{y}} = -\frac{1}{\tilde{\rho}}\frac{\partial \tilde{P}}{\partial \tilde{x}} + \frac{1}{\tilde{\rho}}\frac{\partial \tilde{T}_{xx}}{\partial \tilde{x}} + \frac{1}{\tilde{\rho}}\frac{\partial \tilde{T}_{xy}}{\partial \tilde{y}} + \tilde{g}S \tag{3.10}$$

$$\frac{\partial \tilde{V}}{\partial \tilde{t}} + \tilde{U}\frac{\partial \tilde{V}}{\partial \tilde{x}} + \tilde{V}\frac{\partial \tilde{V}}{\partial \tilde{y}} = -\frac{1}{\tilde{\rho}}\frac{\partial \tilde{P}}{\partial \tilde{y}} + \frac{1}{\tilde{\rho}}\frac{\partial \tilde{T}_{yx}}{\partial \tilde{x}} + \frac{1}{\tilde{\rho}}\frac{\partial \tilde{T}_{yy}}{\partial \tilde{y}} - \tilde{g} \tag{3.11}$$

Continuity equation

$$\frac{\partial \tilde{U}}{\partial \tilde{x}} + \frac{\partial \tilde{V}}{\partial \tilde{y}} = 0 \tag{3.12}$$

where $\tilde{x}$ and $\tilde{y}$ are the stream-wise and normal to the stream-wise direction respectively. $\tilde{U}$ and $\tilde{V}$ are the components of the velocity in the river flow in $\tilde{x}$ and $\tilde{y}$ directions respectively, *S,* $\tilde{P}$,

$\tilde{\rho}$ *and* $\tilde{T}_{ij}$ $(i, j = \tilde{x}, \tilde{y})$ are the average bed slope, the pressure, density of water and the Reynolds stress tensor respectively. The Reynolds stress tensor is expressed as the equations (3.13) and (3.14).

$$(\tilde{T}_{xx}, \tilde{T}_{yy}) = 2\tilde{\rho}\tilde{\nu}_T \left(\frac{\partial \tilde{U}}{\partial \tilde{x}}, \frac{\partial \tilde{V}}{\partial \tilde{y}} \right) \tag{3.13}$$

$$(\tilde{T}_{xy} = \tilde{T}_{yx}) = \tilde{\rho}\tilde{\nu}_T \left(\frac{\partial \tilde{U}}{\partial \tilde{y}} + \frac{\partial \tilde{V}}{\partial \tilde{x}} \right) \tag{3.14}$$

3.2.1 Non-Dimensionalization

The following (3.15) – (3.21) non-dimensionalization terms are used to make the governing equations in non-dimensional manner.

$$(\tilde{x}, \tilde{y}) = \tilde{H}_n (x, y) \tag{3.15}$$

$$(\tilde{U}, \tilde{V}) = \tilde{U}_{fn} (U, V) \tag{3.16}$$

$$(\tilde{P}, \tilde{T}_{ij}) = \tilde{\rho}\tilde{U}_{fn}^{\ 2} (P, T_{ij}) \tag{3.17}$$

$$\tilde{U}_{fn} = \sqrt{\tilde{g}\,\tilde{H}_n\, S} \text{ (shear velocity at normal flow)} \tag{3.18}$$

$$\tilde{t} = \frac{\tilde{H}_n}{\tilde{U}_{fn}} t \tag{3.19}$$

$$(\tilde{H}, \tilde{l}, \tilde{R}) = \tilde{H}_n (H, l, R) \tag{3.20}$$

$$\tilde{\nu}_T = \tilde{U}_{fn}\, \tilde{H}_n (\nu_T) \tag{3.21}$$

3.2.2 Non-Dimensional Manner of the River Flow Governing Equations

By substituting above (3.15) – (3.21) non-dimensionalization forms the governing equations (3.10) – (3.12) are re-written as follows.

$$\frac{\partial U}{\partial t} + U\frac{\partial U}{\partial x} + V\frac{\partial U}{\partial y} = -\frac{\partial P}{\partial x} + \frac{\partial T_{xx}}{\partial x} + \frac{\partial T_{xy}}{\partial y} + 1 \tag{3.22}$$

$$\frac{\partial V}{\partial t} + U\frac{\partial V}{\partial x} + V\frac{\partial V}{\partial y} = -\frac{\partial P}{\partial y} + \frac{\partial T_{yx}}{\partial x} + \frac{\partial T_{yy}}{\partial y} - \frac{1}{S} \tag{3.23}$$

$$\frac{\partial U}{\partial x} + \frac{\partial V}{\partial y} = 0 \tag{3.24}$$

The time scale for the river flow is extremely small with the comparison of it in the seepage layer flow and it has been abolished from the governing equations. Then the non-dimensional governing equations (3.22) – (3.23) are reduced to the following (3.25) – (3.26) equations.

$$U\frac{\partial U}{\partial x}+V\frac{\partial U}{\partial y}=-\frac{\partial P}{\partial x}+\frac{\partial T_{xx}}{\partial x}+\frac{\partial T_{xy}}{\partial y}+1 \tag{3.25}$$

$$U\frac{\partial V}{\partial x}+V\frac{\partial V}{\partial y}=-\frac{\partial P}{\partial y}+\frac{\partial T_{yx}}{\partial x}+\frac{\partial T_{yy}}{\partial y}-\frac{1}{S} \tag{3.26}$$

By the use of mixing length turbulent model for open channel flow, the Reynolds stress tensor is written as follows *[2]*.

$$(T_{xx},T_{yy})=2\nu_T\left(\frac{\partial U}{\partial x},\frac{\partial V}{\partial y}\right) \tag{3.27}$$

$$(T_{xy}=T_{yx})=\nu_T\left(\frac{\partial U}{\partial y}+\frac{\partial V}{\partial x}\right) \tag{3.28}$$

$$\nu_T=l^2\frac{\partial U}{\partial y} \tag{3.29}$$

$$l=\kappa(y+R)\sqrt{\frac{H-y}{H}} \tag{3.30}$$

where ν_T, l, H and R are the eddy viscosity, mixing length, the flow depth and the reference level at which the velocity vanishes in the logarithmic velocity distribution respectively, and κ is the Karman constant which is considered to be 0.4 in this analysis.

3.3 DIMENSIONAL MANNER OF THE SEEPAGE FLOW GOVERNING EQUATIONS

Seepage flow is expressed using the Brinkman-Forchheimer equations *[4]* and the continuity equation.

Stream-wise direction - ($\tilde{x}$)

$$\frac{1}{\lambda}\frac{\partial\tilde{u}}{\partial\tilde{t}}+\frac{1}{\lambda^2}\tilde{u}\frac{\partial\tilde{u}}{\partial\tilde{x}}+\frac{1}{\lambda^2}\tilde{v}\frac{\partial\tilde{u}}{\partial\tilde{y}}=-\frac{1}{\tilde{\rho}}\frac{\partial\tilde{p}}{\partial\tilde{x}}+\frac{1}{\tilde{\rho}}\frac{\partial\tilde{\tau}_{xx}}{\partial\tilde{x}}+\frac{1}{\tilde{\rho}}\frac{\partial\tilde{\tau}_{xy}}{\partial\tilde{y}}+\tilde{g}S-\frac{\tilde{\mu}}{\tilde{\rho}\tilde{K}}\tilde{u}-\frac{c_F}{\sqrt{\tilde{K}}}\tilde{u}\sqrt{\tilde{u}^2+\tilde{v}^2} \tag{3.31}$$

Normal to stream-wise direction – ($\tilde{y}$)

$$\frac{1}{\lambda}\frac{\partial\tilde{v}}{\partial\tilde{t}}+\frac{1}{\lambda^2}\tilde{u}\frac{\partial\tilde{v}}{\partial\tilde{x}}+\frac{1}{\lambda^2}\tilde{v}\frac{\partial\tilde{v}}{\partial\tilde{y}}=-\frac{1}{\tilde{\rho}}\frac{\partial\tilde{p}}{\partial\tilde{y}}+\frac{1}{\tilde{\rho}}\frac{\partial\tilde{\tau}_{yx}}{\partial\tilde{x}}+\frac{1}{\tilde{\rho}}\frac{\partial\tilde{\tau}_{yy}}{\partial\tilde{y}}-\tilde{g}-\frac{\tilde{\mu}}{\tilde{\rho}\tilde{K}}\tilde{v}-\frac{c_F}{\sqrt{\tilde{K}}}\tilde{v}\sqrt{\tilde{u}^2+\tilde{v}^2} \tag{3.32}$$

Continuity equation

$$\frac{\partial \tilde{u}}{\partial \tilde{x}} + \frac{\partial \tilde{v}}{\partial \tilde{y}} = 0 \tag{3.33}$$

$\tilde{u}$ and $\tilde{v}$ are the components of the virtual velocity in the seepage layer in $\tilde{x}$ and $\tilde{y}$ directions respectively, $\tilde{p}$ *and* $\tilde{\tau}_{ij}$ $(i, j = \tilde{x}, \tilde{y})$ are the pressure in the seepage layer and the stress tensor respectively. $\tilde{\mu}$ and λ are the viscosity of water and the porosity of the seepage layer respectively. Here the non-dimensional equations are not shown, since the base state solution for the seepage layer is only important to the analysis. Under the subtitle base state solutions the non-dimensional equations are shown.

3.4 BOUNDARY CONDITIONS

3.4.1 Dynamic Boundary Conditions at the Water Surface of the River Flow Layer $(y = H)$

Tangential and normal stresses are vanished and they can be expressed as follows.

$$e_{ts}.T.e_{ns} = 0 \tag{3.34}$$

$$e_{ns}.T.e_{ns} = 0 \tag{3.35}$$

where e_{ts} and e_{ns} are the unit vectors in the directions tangential and normal to the water surface respectively, which can be written in the following forms

$$e_{ts} = \frac{1, \partial H/\partial x}{\sqrt{1+\left(\partial H/\partial x\right)^2}} \tag{3.36}$$

$$e_{ns} = \frac{-\partial H/\partial x, 1}{\sqrt{1+\left(\partial H/\partial x\right)^2}} \tag{3.37}$$

and T is the stress tensor expressed as

$$T = \begin{bmatrix} -P + T_{xx} & T_{xy} \\ T_{xy} & -P + T_{yy} \end{bmatrix} \tag{3.38}$$

3.4.2 Kinematics Boundary Conditions at the Water Surface of the River Flow Layer $(y = H)$

Kinematics boundary condition is obtained as follows.

$$\frac{D(H)}{Dt} = V(H) = \frac{\partial H}{\partial t} + U\frac{\partial H}{\partial x} + V\frac{\partial H}{\partial y} \tag{3.39}$$

$\frac{\partial H}{\partial t} \to 0$ Time derivative terms are neglected

$V\frac{\partial H}{\partial y} \to 0$ No flow in y direction at the surface

Therefore the boundary condition equation (3.39) is reduced to the (3.40).

$$V(H) = U\frac{\partial H}{\partial x} \tag{3.40}$$

3.4.3 Matching Conditions at the Boundary of the River Layer and the Seepage Layer $(y = 0)$

It is assumed that the slip velocity for the free fluid is proportional to the shear rate at the permeable boundary *[5]*.

$$\frac{\partial U}{\partial y} = \frac{\alpha}{\sqrt{K}}\left(U_B - \bar{u}\right) \tag{3.41}$$

Value of α for water is around 0.8 to 1.2 according to Gordon et al *[5]* and it is assumed to be $\alpha = 1.0$ for this analysis. Then the above (3.41) equation is re-written as (3.42).

$$\frac{\partial U}{\partial y} = \frac{1}{\sqrt{K}}\left(U_B - \bar{u}\right) \tag{3.42}$$

where U_B is horizontal velocity at the bed of the river layer $(y = 0)$ and $\bar{u}$ is the assumed uniform constant velocity in the stream-wise direction of the seepage layer and K is the non-dimensional permeability of the seepage layer.

It is also assumed that the normal component of the velocity and the pressure are continuous at the porous boundary *[5]*. The depth average continuity equation for the seepage flow is shown as follows.

$$\int_{-h}^{0} \frac{\partial \bar{u}}{\partial x} dy + \int_{-h}^{0} \frac{\partial v}{\partial y} dy = 0 \tag{3.43}$$

The first portion of the equation (3.43) is expanded as follows

$$\int_{-h}^{0} \frac{\partial \bar{u}}{\partial x} dy = \frac{d}{dx} \int_{-h}^{0} \bar{u} dy$$

$$\int_{-h}^{0} \frac{\partial \bar{u}}{\partial x} dy = \frac{d}{dx} \int_{-h}^{0} \bar{u} dy = \frac{d\bar{u}h}{dx} = h\frac{\partial \bar{u}}{\partial x} \tag{3.44}$$

The second portion of the equation (3.43) is expanded as follows.

$$\int_{-h}^{0} \frac{\partial v}{\partial y} dy = v(0) - v(-h)$$

where h is the non-dimensional depth of the seepage layer. Normal velocity at the bottom of the seepage layer is assumed to be vanished and the following information can be written.

$v(-h) \to 0$

Then the second part is reduced to the following (3.45) equation.

$$\int_{-h}^{0} \frac{\partial v}{\partial y} dy = v(0) \tag{3.45}$$

Combing (3.44) and (3.45) equations, the depth average continuity equation (3.43) can be re-written as the following.

$$h\frac{\partial \bar{u}}{\partial x} + v(0) = 0 \tag{3.46}$$

3.5 BASE STATE SOLUTIONS

3.5.1 Base State Solution for the River Flow

The base state solution for river flow without disturbances is obtained here. River flow is assumed to be steady. The derivative terms with respect to x can be ignored. Flow is only in x direction and the terms with V can also be ignored from the governing equations.

Stream-wise directional governing equation (3.25) is considered in order to obtain the base state solutions for the river flow.

$$U\frac{\partial U}{\partial x}+V\frac{\partial U}{\partial y}=-\frac{\partial P}{\partial x}+\frac{\partial T_{xx}}{\partial x}+\frac{\partial T_{xy}}{\partial y}+1$$

This equation is reduced to the equation (3.47) with the above mentioned conditions.

$$0=\frac{\partial T_{xy}}{\partial y}+1$$

$$\frac{\partial T_{xy}}{\partial y}=-1 \tag{3.47}$$

Reynolds stress tensor from equation (3.28) can be reduced to the following equation (3.48) at the base state solutions.

$$T_{xy}=\nu_T\left(\frac{\partial U}{\partial y}+\frac{\partial V}{\partial x}\right),\frac{\partial V}{\partial x}\to 0$$

$$T_{xy}=\nu_T\frac{\partial U}{\partial y} \tag{3.48}$$

Mixing length equation (3.30) is also reduced to equation (3.49).

$$l=\kappa(y+R)\sqrt{1-y}\;;\; H\to 1 \tag{3.49}$$

By integrating the equation (3.47) with respect to y, it can be found the following.

$$T_{xy}=-y+C_1$$

At bed it is assumed that $T_{xy}=1$ and therefore $C_1=1$

Then;

$$T_{xy}=1-y \tag{3.50}$$

From equations (3.48), (3.50) and (3.29) the following combination can be found.

$$\frac{\partial U}{\partial y}=\frac{1}{\kappa(y+R)} \tag{3.51}$$

The logarithmic velocity distribution (3.52) can be found by integrating the above (3.51) equation with respect to y.

$$U = \frac{1}{\kappa}\ln(y+R) + C_2 \tag{3.52}$$

Using the boundary and matching conditions value of C_2 is found as the followings.

At $y = 0$ (3.51) equation can be reduced to the following.

$$\frac{\partial U_B}{\partial y} = \frac{1}{\kappa R} \tag{3.53}$$

From the matching conditions at the bottom of the river flow layer; (3.42) and (3.53) U_B can be found as the following.

$$U_B = \bar{u} + \frac{\sqrt{K}}{\kappa R} \tag{3.54}$$

With the above solution, value of C_2 can be found as follows using the equation (3.52).

At $y = 0$

$$C_2 = U_B - \frac{1}{\kappa}\ln R \tag{3.55}$$

Then, the logarithmic velocity distribution of the river layer can be found by combing above (3.52) and (3.55) equations as follows.

$$U = \frac{1}{\kappa}\ln\left(\frac{y+R}{R}\right) + \bar{u} + \frac{\sqrt{K}}{\kappa R} \tag{3.56}$$

3.5.2 Base State Solution for Seepage Flow Layer

Stream-wise direction governing equation (3.31) is considered at this state and the following assumptions are assumed to obtain the base state solution for the seepage flow.

- Shallow water approximation – no shear
- Horizontal velocity in the seepage layer is uniform in the depth direction
- Vertical velocity in the seepage layer is neglected

Equation (3.31) can be reduced at the base state as follows with the above assumptions.

$$\frac{1}{\lambda}\frac{\partial \tilde{u}}{\partial \tilde{t}}+\frac{1}{\lambda^2}\tilde{u}\frac{\partial \tilde{u}}{\partial \tilde{x}}+\frac{1}{\lambda^2}\tilde{v}\frac{\partial \tilde{u}}{\partial \tilde{y}}=-\frac{1}{\tilde{\rho}}\frac{\partial \tilde{p}}{\partial \tilde{x}}+\frac{1}{\tilde{\rho}}\frac{\partial \tilde{\tau}_{xx}}{\partial \tilde{x}}+\frac{1}{\tilde{\rho}}\frac{\partial \tilde{\tau}_{xy}}{\partial \tilde{y}}+\tilde{g}S-\frac{\tilde{\mu}}{\tilde{\rho}\tilde{K}}\tilde{u}-\frac{c_F}{\sqrt{\tilde{K}}}\tilde{u}\sqrt{\tilde{u}^2+\tilde{v}^2}$$

$$0=\tilde{g}S-\frac{\tilde{\mu}}{\tilde{\rho}\tilde{K}}\tilde{u}-\frac{c_F}{\sqrt{\tilde{K}}}\tilde{u}\sqrt{\tilde{u}^2+\tilde{v}^2} \tag{3.57}$$

The following non-dimensionalization terms are introduced in order to get the non-dimensional stream-wise directional equation of the base state in the seepage layer.

$$(\tilde{u},\tilde{v})=\tilde{U}_r(u,v) \tag{3.58}$$

$$\tilde{p}=\tilde{\rho}\tilde{U}_{fn}^{\ 2}\ p \tag{3.59}$$

$$\tilde{U}_r=\frac{\tilde{\rho}\tilde{g}S\tilde{K}}{\tilde{\mu}} \tag{3.60}$$

$$\tilde{\mu}=\tilde{\rho}\tilde{U}_{fn}\tilde{H}_n\,\mu \tag{3.61}$$

$$\tilde{K}=\tilde{H}_n^{\ 2}\ K \tag{3.62}$$

$$\tilde{t}=\tilde{T}t \tag{3.63}$$

$$\tilde{T}=\frac{\tilde{U}_r}{\lambda\tilde{g}S} \tag{3.64}$$

where $\tilde{U}_r$ is well smaller than $\tilde{U}_{fn}$ and the time scale for the seepage flow, $\tilde{T}$ is well higher than the time scale of river flow. By substituting the above mentioned non-dimensionalization terms to the equation (3.57) the following non-dimensional stream-wise directional equation is obtained as follows.

$$0=1-\bar{u}-\frac{c_F\bar{u}^2K^{3/2}}{\mu^2} \tag{3.65}$$

Base sate solution of the seepage flow is given by the solution of the equation (3.65) and shown as follows.

$$\bar{u}=\frac{-\mu^2\pm\sqrt{\mu^4+4c_FK^{3/2}}}{2c_FK^{3/2}}$$

However the negative solution is ignored since the velocity in the seepage layer should be physically positive or in the stream-wise direction in order to implement this analysis.

$$\bar{u} = \frac{-\mu^2 + \sqrt{\mu^4 + 4c_F K^{3/2}}}{2c_F K^{3/2}} \tag{3.66}$$

3.6 LINEAR STABILITY ANALYSIS

Stream function is introduced to the river flow governing equations to reduce the two unknown velocity components to one unknown parameter as follows.

$$(U,V) = \left(\frac{\partial \Psi}{\partial y}, -\frac{\partial \Psi}{\partial x}\right) \tag{3.77}$$

By substituting equation (3.77) into (3.25) and (3.26), the following forms of the governing equations are obtained.

Stream-wise direction - ($\tilde{x}$)

$$\frac{\partial \Psi}{\partial y}\frac{\partial^2 \Psi}{\partial x \partial y} - \frac{\partial \Psi}{\partial x}\frac{\partial^2 \Psi}{\partial y^2} + \frac{\partial P}{\partial x} - \frac{\partial}{\partial x}\left(2\nu_T \frac{\partial^2 \Psi}{\partial x \partial y}\right) + \frac{\partial}{\partial y}\left(\nu_T\left(\frac{\partial^2 \Psi}{\partial x^2} - \frac{\partial^2 \Psi}{\partial y^2}\right)\right) - 1 = 0 \tag{3.78}$$

Normal to stream-wise direction – ($\tilde{y}$)

$$-\frac{\partial \Psi}{\partial y}\frac{\partial^2 \Psi}{\partial x^2} + \frac{\partial \Psi}{\partial x}\frac{\partial^2 \Psi}{\partial x \partial y} + \frac{\partial P}{\partial y} + \frac{\partial}{\partial x}\left(\nu_T\left(\frac{\partial^2 \Psi}{\partial x^2} - \frac{\partial^2 \Psi}{\partial y^2}\right)\right) + \frac{\partial}{\partial y}\left(2\nu_T \frac{\partial^2 \Psi}{\partial x \partial y}\right) + \frac{1}{S} = 0 \tag{3.79}$$

Subtracting the y derivative of the equation (3.78) from the x derivative of the equation (3.79), the pressure term can be eliminated from the governing equation and it is shown as follows.

$$\frac{\partial \Psi}{\partial y}\left(\frac{\partial^3 \Psi}{\partial x \partial y^2} - \frac{\partial^3 \Psi}{\partial x^3}\right) - \frac{\partial \Psi}{\partial x}\left(\frac{\partial^3 \Psi}{\partial y^3} + \frac{\partial^3 \Psi}{\partial x^2 \partial y}\right) - 4\frac{\partial^2}{\partial x \partial y}\left(\nu_T \frac{\partial^2 \Psi}{\partial x \partial y}\right) + \left(\frac{\partial^2}{\partial y^2} - \frac{\partial^2}{\partial x^2}\right)\left(\nu_T\left(\frac{\partial^2 \Psi}{\partial x^2} - \frac{\partial^2 \Psi}{\partial y^2}\right)\right) = 0 \tag{3.80}$$

The following mathematical symbol is used by the author to reduce the above equation (3.80).

$$\nabla = \frac{\partial^2}{\partial x^2} + \frac{\partial^2}{\partial y^2} \tag{3.81}$$

Substituting this mathematical symbol to equation (3.80), the following reduced equation is obtained.

$$\frac{\partial \Psi}{\partial y}\frac{\partial \nabla^2 \Psi}{\partial x} - \frac{\partial \Psi}{\partial x}\frac{\partial \nabla^2 \Psi}{\partial y} - 4\frac{\partial^2}{\partial x \partial y}\left(\nu_T \frac{\partial^2 \Psi}{\partial x \partial y}\right) + \left(\frac{\partial^2}{\partial y^2} - \frac{\partial^2}{\partial x^2}\right)\left(\nu_T\left(\frac{\partial^2 \Psi}{\partial x^2} - \frac{\partial^2 \Psi}{\partial y^2}\right)\right) = 0 \tag{3.82}$$

Important variables are expanded using equation (3.83) to get the perturbation solution

$$\left(\Psi, P, H, \overline{u}\right) = \left(\Psi_0, P_0, 1, \overline{u_0}\right) + A\left(\hat{\Psi}_1, \hat{P}_1, \hat{H}_1, \hat{\overline{u}}_1\right) \tag{3.83}$$

$$\left(\hat{\Psi}_1, \hat{P}_1, \hat{H}_1, \hat{\overline{u}}_1\right) = \left(\Psi_1(y), P_1(y), H_1, \overline{u_1}\right) e^{i(kx - \omega t)} + C.C. \tag{3.84}$$

where A is the amplitude of the perturbation, which is an infinitesimally small, k and ω are the wave number and the complex angular frequency of the perturbation, respectively. The perturbations are expressed by the Fourier series and C.C. is the complex conjugate of the preceding term.

Then the governing equation (3.80), matching conditions and boundary conditions are expanded with respect to A using equations (3.83) and (3.84). But the boundary condition (3.34) eliminated as it is always satisfied because the eddy viscosity ν_T always vanishes at the water surface. However the other boundary and matching conditions which are denoted by (3.35), (3.40), (3.42) and (3.46) are expanded with respect to A.

3.7 NUMERICAL SOLUTION

Expanded governing equation (3.80) is solved using the expanded boundary and matching conditions with use of spectral collocation method incorporated with Chebyshev polynomials. In order to do that, the stream function is expanded by Chebyshev polynomials in the following form.

$$\Psi_1 = \sum_{j=0}^{n} a_j T_j(\xi) \tag{3.85}$$

where T_j is the j^{th} term of the Chebyshev polynomials and ξ is a variable of the Chebyshev polynomials defined in the range of $[-1 \le \xi \le 1]$. Then the river flow layer $[0 \le y \le 1]$ is transformed in the range of $[-1 \le \xi \le 1]$ by the following transformation.

$$\xi[y\_] = 2\frac{\ln(y + R/R)}{\ln(1 + R/R)} - 1 \tag{3.86}$$

After introducing the above equations, Gauss-Labatt points are evaluated in the following form.

$$\xi_j = \cos\frac{j\Pi}{n}; j = (0,1,...,n) \tag{3.87}$$

Then, the expanded governing equation and expanded boundary and matching conditions are obtained at the above mentioned Gauss-Labatt points. These equations can be simply shown in the matrix form as follows.

$$\overline{A}a = \omega\overline{B}a \tag{3.88}$$

where a can be denoted as follows

$$a = \left[a_0, a_1, ...a_{n,} H_1\right] \tag{3.89}$$

$\overline{A}$ and $\overline{B}$ are two square matrices in $(n+1)\times(n+1)$ size. In this analysis numerical value of n is taken to be 30. The above (3.88) matrix equation forms a generalized eigenvalue problem with the eigen-value ω; which is a function of several parameters as follows.

$$\omega = \omega(k, S, D_P, R, K, \lambda) \tag{3.90}$$

where k and D_P are the non-dimensional wave number and the non-dimensional particle diameter of the bed material. The dimensional particle diameter $\tilde{d}_P$ is non-dimensionalized using the following combination.

$$D_P = \frac{\tilde{d}_P}{\tilde{H}_n} \tag{3.91}$$

The imaginary part of ω corresponds to the growth rate of the perturbation and the real part represents the phase velocity of the wave. In order to obtain the numerical solution, values for the porosity of the porous matrix (λ) and the reference level where the logarithmic velocity distribution vanishes (R) are assumed as follows.

$$\lambda = 0.6 \tag{3.92}$$

$$R = \frac{2.5 D_P}{30} \tag{3.93}$$

3.8 RESULTS OF THE LINEAR STABILITY ANALYSIS

It has been understood that the particle diameter of the sediments and the longitudinal slope of the river and seepage layer are two most important factors to the hyporheic interactions *[1] and [3]*. Therefore, the analysis is carried out for three slopes of the combined river flow and seepage flow layers as 0.01%, 0.1% and 1%. Also the growth rate contours are plotted in the dimensionless particle diameter (D_P) and wave number (k) axes system. Figure 3.2 - Figure 3.4 show the imaginary part of the growth rate of perturbation as a function of dimensionless particle diameter and the wave number when the slopes are 0.01%, 0.1% and 1% respectively. These instability diagrams are obtained at the small wave numbers. Span of the vertical axis is considered, in order to address the real situation. The particle diameter should be small enough with the height of the river flow layer. Therefore the particle diameter is considered to be one tenth of the river water depth as the maximum. Considered dimensionless particle diameter is in a range of 0.001 to 0.1.

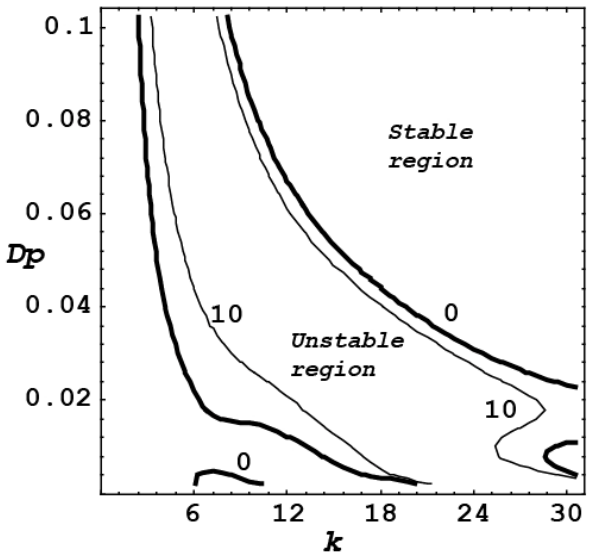

Figure 3.2 Imaginary part of the growth rate contours of the perturbations S = 0.01% with small wave numbers

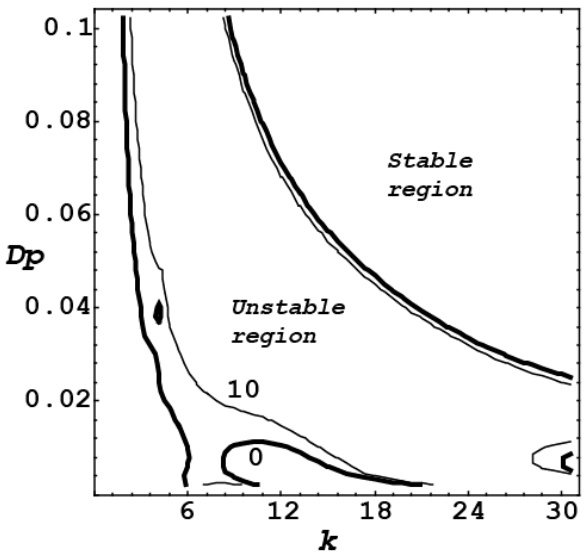

Figure 3.3 Imaginary part of the growth rate contours of the perturbations S = 0.1% with small wave numbers

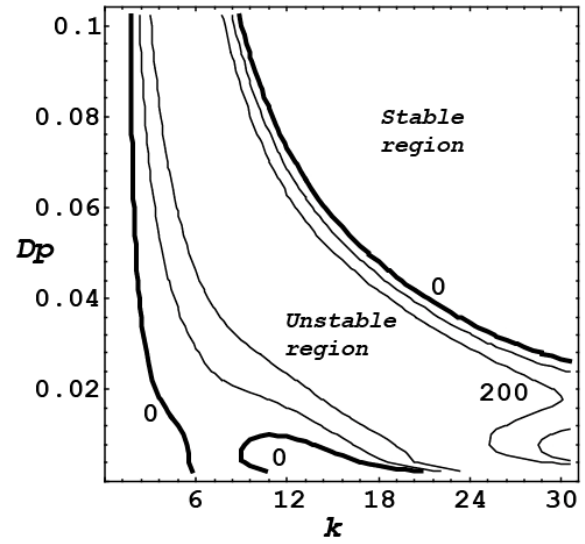

Figure 3.4 Imaginary part of the growth rate contours of the perturbations S = 1% with small wave numbers

From the theoretical analysis another instability region is found in each and every slope, when the wave numbers are in the range of 150 to 1000 and the imaginary part of the growth rate contours of the perturbations are shown at 0.01%, 0.1% and 1% slopes respectively by Figure 3.5, Figure 3.6 and Figure 3.7 as follows.

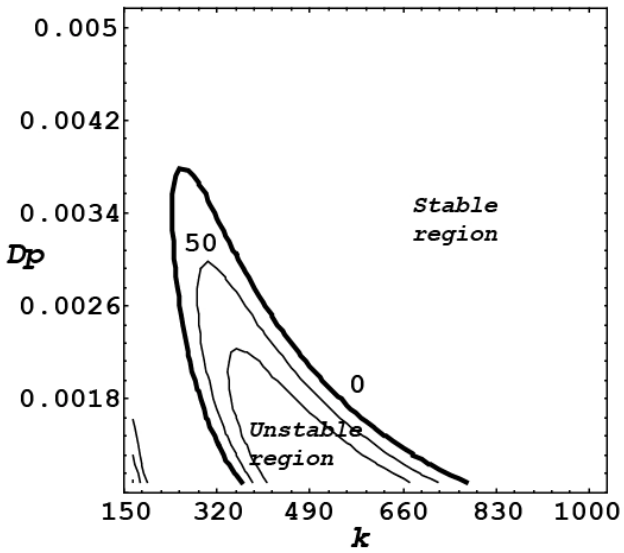

Figure 3.5 Imaginary part of the growth rate contours of the perturbations S = 0.01% with large wave numbers

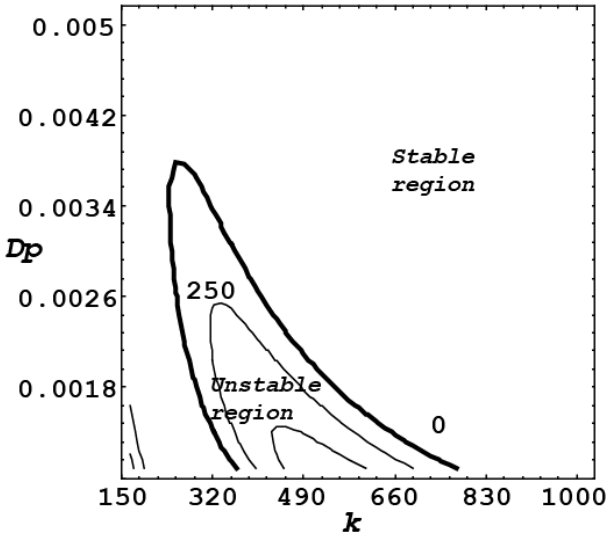

Figure 3.6 Imaginary part of the growth rate contours of the perturbations S = 0.1% with large wave numbers

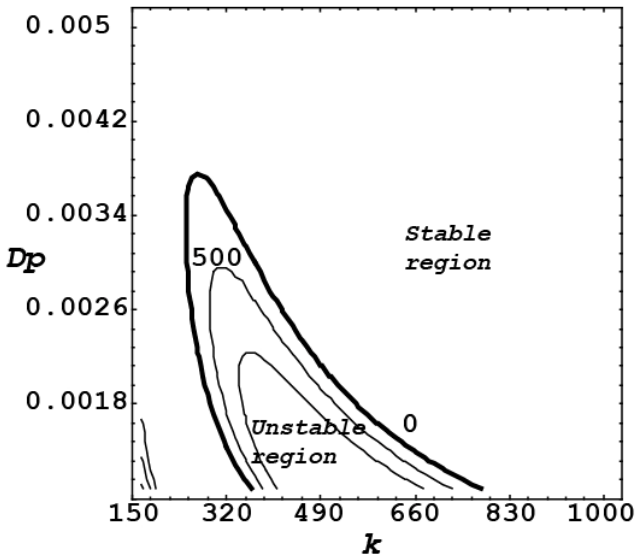

Figure 3.7 Imaginary part of the growth rate contours of the perturbations S = 1% with large wave numbers

3.9 DISCUSSION AND CONCLUSIONS

The thick black lines of Figure 3.2 – Figure 3.7 show the neutral curves, where the growth rate of imaginary part is zero. Inside the neutral curve growth rate is positive and this means that the growth rate of the perturbation that we have introduced increases. Therefore, it can be learnt that the normal flow is unstable in side the neutral curves. This means that the instability occurs among the river flow and seepage layers in side the neutral curve at the shown wave numbers and the dimensionless particle diameters.

Out side the neutral curve, the growth rate is negative and this means that the growth rate of the small perturbation decreases. Therefore it can be learnt that the normal flow is stable and instability is not occurred out side of the neutral curve.

It is important to recognize one more instability region when the wave numbers are comparably high as shown in Figure 3.5 – Figure 3.7. This means that the wave lengths are quite small and interactions are occurred at small wave lengths. Even though it is quite strange, the theoretical results should be further understood through an experimental study. However some literature has mentioned that the hyporheic interactions can be occurred even in small wave lengths such as 5 cm in the real case *[6]*.

By comparison, the Figure 3.2 – Figure 3.4, it can be clearly noted that the range for the occurrence of instability region increases with the slope. However, this interesting process cannot be understood from the Figure 3.5 – Figure 3.7. Therefore, it can be concluded that the hyporheic interactions are improved with the slope when the wave numbers are small enough or else the wave lengths are large.

REFERENCES

[1]Boulton A.J., Findlay S., Marmonier P., Stanley E.H. and Valett H.M., The functional significance of the hyporheic zone in streams and rivers, *Annual Review of Ecology and Systematic*, 29, 59-81, 1998

[2]Colombini M., Revisiting the linear theory of sand dune formation, *Journal of Fluid Mechanics*, 502, 1-16, 2004

[3]Daniele Tonina and M. Buffington, Hyporheic exchange in gravel bed rivers with pool-riffle morphology; Laboratory experiments and three dimensional modeling, *Journal of Water Resources Research*, 43, 2007

[4]Derek B. Ingham and Iioan Pop, Transport phenomena in porous media II, 1st Edition, *Elsevier Science Ltd*, ISBN: 0-08-043965-9, 2002

[5]Gordon S. Beavers and Daniel D. Joseph, Boundary conditions at a natural permeable wall, *Journal of Fluid Mechanics*, 30, 197-207, 1967

[6]Harvey J.W. and Wagner B.J., Quantifying hydrologic interactions between streams and their subsurface hyporheic zones, *Streams and ground waters*, Jones J.B. and Mulholland P.J., (Editors), Academic Press, San Diego, USA, pp 197-220, 2000

Chapter 4

EXPERIMENTS FOR THE RIVER FLOW AND SEEPAGE FLOW INTERACTIONS

4.1 INTRODUCTION

In order to understand the hyporheic interactions (river water and seepage water interactions) a set of experiments are carried out. However the seepage layer is experimentally modeled using a Hele-Shaw model. The details of the experimental set up can be found from the Figure 4.1, which is not drawn to a scale. Hele-Shaw model is placed inside the channel and the longitudinal section, the sectional view and plan view of the Hele-Shaw model is shown in the Figure 4.2.

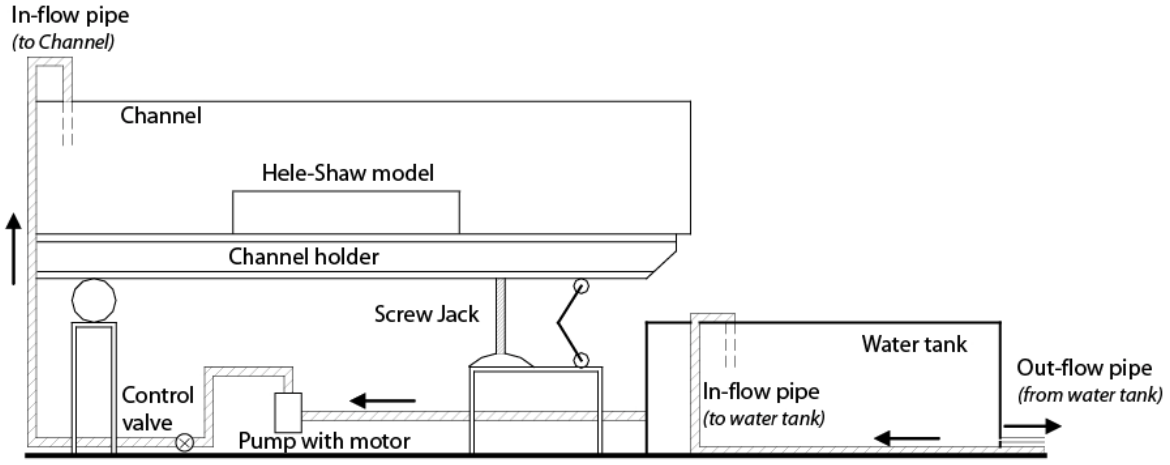

Figure 4.1 Experimental set up

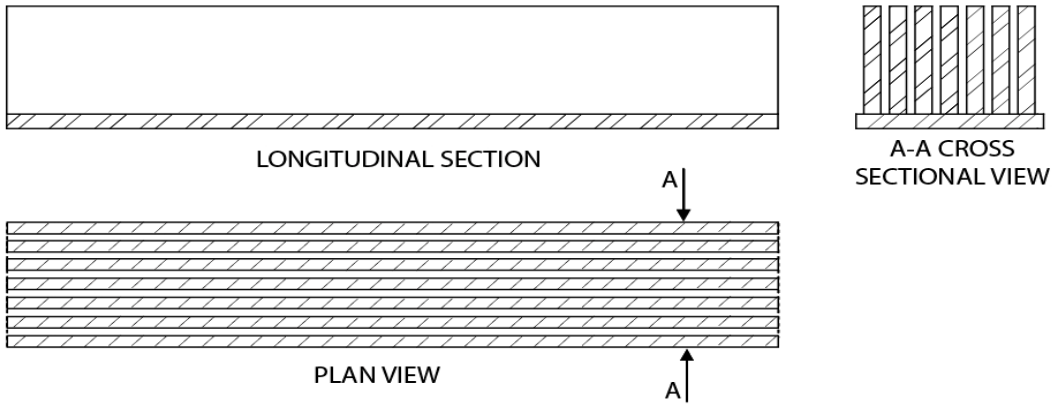

Figure 4.2 Hele-Shaw model

4.2 DIMENSIONS OF THE EXPERIMENTAL SET UP

The re-circulating channel is used in this work, has a section of 5 m in length and a channel width of 20 cm. The channel is 40 cm in depth and flexible to change its slope using the screw jack at right edge. It is made up of transparent materials, which allows direct observations of interactions and managed to have digital pictures and digital movies. Let us consider $\tilde{x}$ co-ordinates of the left edge of the channel is to be 0 m and the right edge of the channel is to be 5.0 m respectively. The Hele-Shaw model, where 2.0 m in length, 20 cm in width and 10 cm in height is placed at $\tilde{x} = 2.1$. The porosity; λ of the Hele-Shaw model is 0.3 in the used set up.

4.3 EXPERIMENTAL WORK

4.3.1 River Flow and Seepage Flow Interactions Visualization

Due to the initiation of a barrier (at $\tilde{x} = 2.1$) because of the Hele-Shaw model in the channel and the back water effect at the end of the weir, all the experimental data are obtained, keeping a clearance at the $\tilde{x} = 2.1$ and $\tilde{x} = 4.1$. Uniform flow is obtained in the channel and it is ensured using three water height measurements at $\tilde{x} = 2.7$, $\tilde{x} = 3.1$ and $\tilde{x} = 3.5$. Experiments are carried out for two slopes as 0.1%, and 0.2%. Combined channel flow height is controlled using a down-stream weir from about 12 cm to about 25 cm. Three trials of experiments with same conditions are carried out for the each river height.

Methylene blue (blue color dye) is injected just downwards and along the upper boundary of the Hele-Shaw model, in order to visualize the seepage flow and river flow interactions. Continuous pictures are taken at 5 s intervals in each and every experiment. In some cases few videos are taken. Best picture which has the clear interactions is digitized using the commercial package “Bytescout Graph Digitizer Scout 1.2.4”. The corresponding wave lengths for S=0.1%, and 0.2% slopes are obtained using these digitized pictures. Few digital pictures are shown in Figure 4.3 – Figure 4.8 in order to verify the flow interactions.

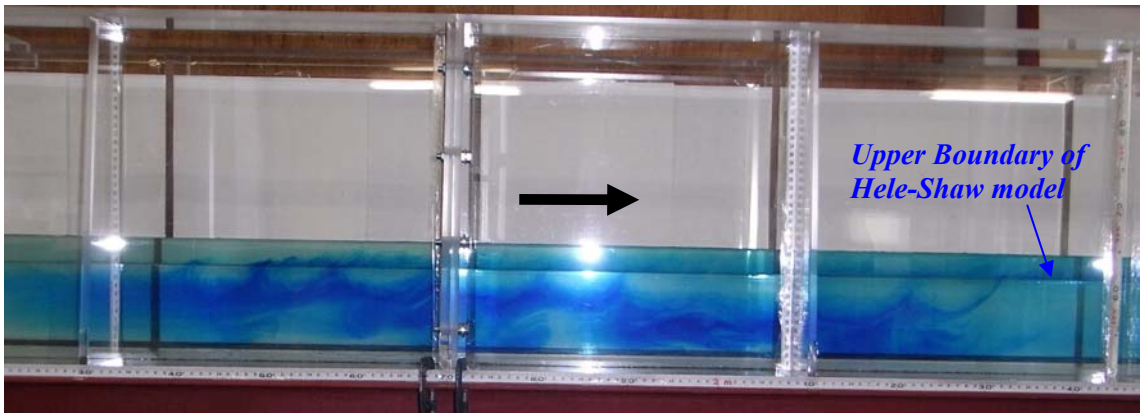

Figure 4.3 Interactions at 0.1% slope when the river height is 3 cm

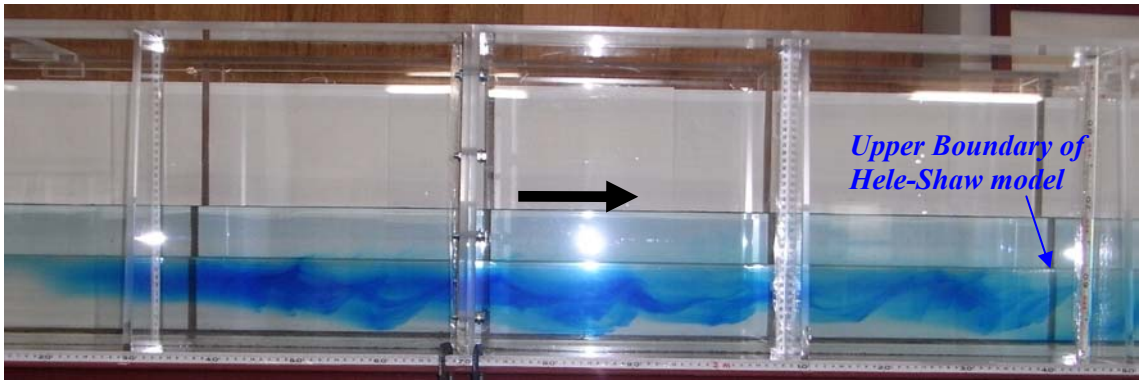

Figure 4.4 Interactions at 0.1% slope when the river height is 6.5 cm

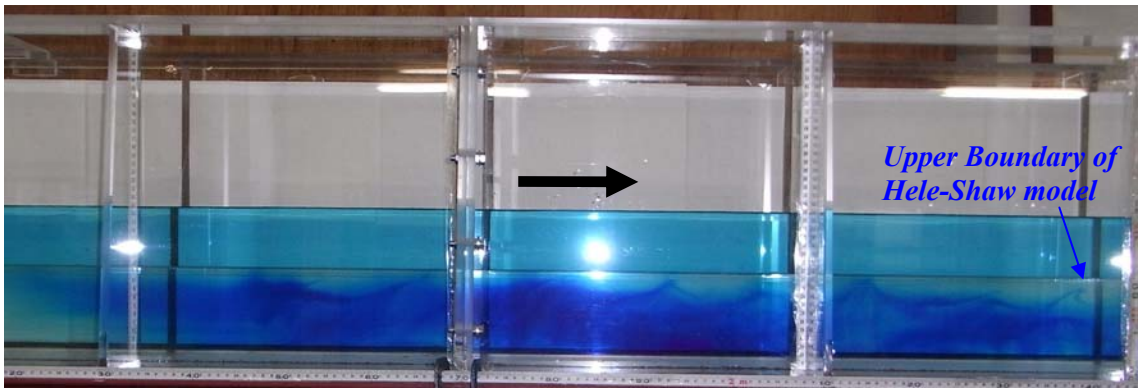

Figure 4.5 Interactions at 0.1% slope when the river height is 7.2 cm

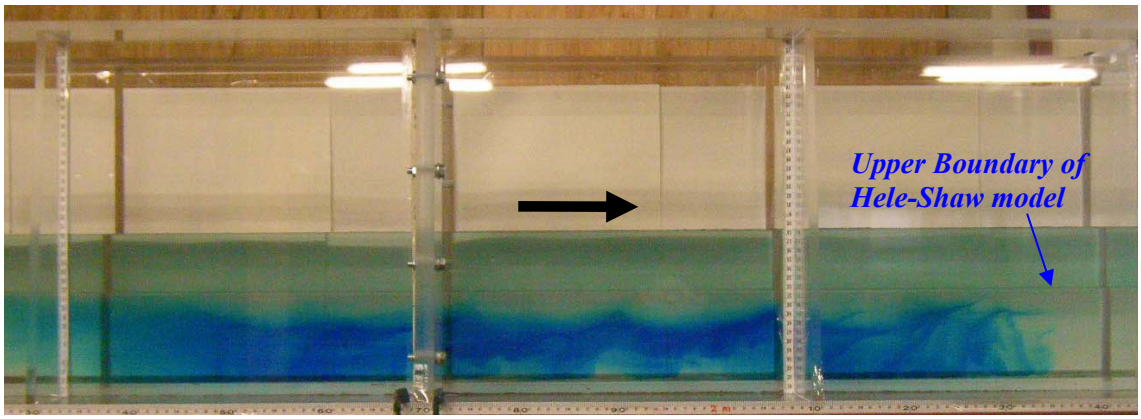

Figure 4.6 Interactions at 0.2% slope when the river height is 6.5 cm

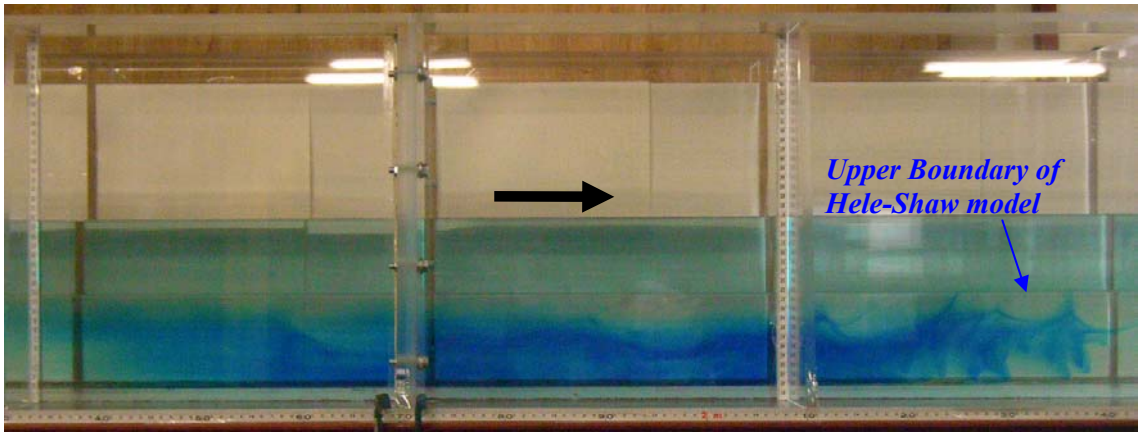

Figure 4.7 Interactions at 0.2% slope when the river height is 8.0 cm

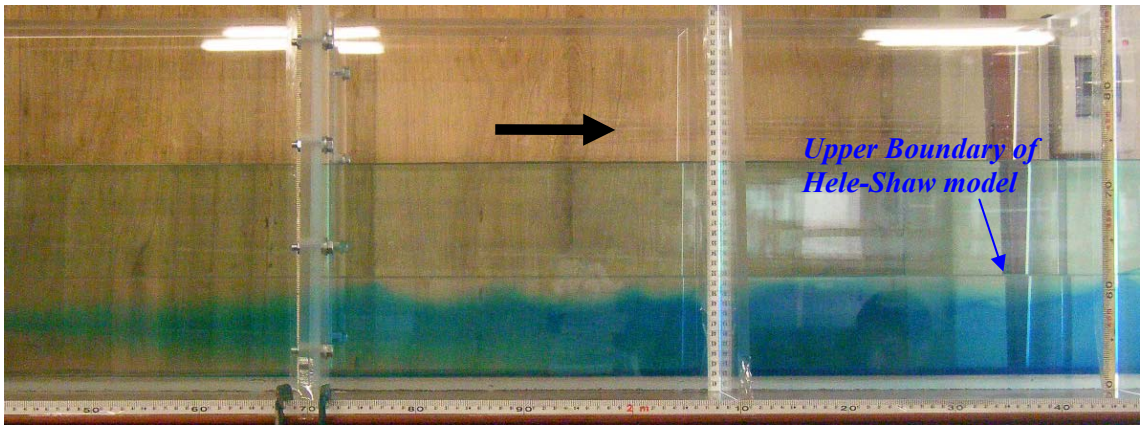

Figure 4.8 Interactions at 0.2% slope when the river height is 11.3 cm

4.4 FROUDE NUMBER FOR THE RIVER FLOW / OPEN CHANNEL FLOW

4.4.1 Average Velocity in the River / Open Channel Flow

Average velocity is calculated using the discharge measurements. Flow in the Hele-Shaw model is neglected in this calculation, since the discharge in the Hele-Shaw model is very small.

$$\overline{\tilde{U}_{avg}} = \frac{\tilde{Q}}{\tilde{Area}} \tag{4.1}$$

$$\overline{\tilde{U}_{avg}} = \frac{\tilde{Q}}{\tilde{H}_n \tilde{B}} \tag{4.2}$$

where $\tilde{Q}$ and $\tilde{B}$ are the dimensional discharge of the open channel and the width of the channel.

4.4.2 Froude Number for the River / Open Channel Flow

Froude number for the river / open channel flow is calculated using the following equation (4.3).

$$Fr = \frac{\overline{\tilde{U}_{avg}}}{\sqrt{g \tilde{H}_n}} \tag{4.3}$$

4.5 RESULTS OF THE EXPERIMENTAL WORK

Obtained wave lengths according to the 0.1% and 0.2% slopes are tabulated as in Table 4.1 and 4.2 respectively. Non-dimensionalization is done using the height of the river layer and the non-dimensional wave number is obtained as follows.

$$k = \frac{2\Pi}{\tilde{L} / \tilde{H}} \tag{4.4}$$

Table 4.1 Dimensionless wave numbers and Froude number at $S = 0.1\%$

Experiment number	River layer height ($\tilde{H}$) / cm	Average wave length ($\tilde{L}$)/ cm	Wave Length / River layer height	Non-Dimensional wave number / k	River Froude Number / Fr
1	3	14.58	4.86	1.29	0.307
2	3	14.34	4.78	1.32	0.307
3	3	11.28	3.76	1.67	0.307
4	4.6	12.00	2.61	2.41	0.324
5	4.6	13.60	2.96	2.13	0.324
6	4.6	12.28	2.67	2.35	0.324
7	6.5	17.03	2.62	2.40	0.213
8	6.5	19.13	2.94	2.14	0.213
9	6.5	20.11	3.09	2.03	0.213
10	7.2	15.05	2.09	3.01	0.215
11	7.2	15.67	2.18	2.89	0.215
12	7.2	14.60	2.03	3.10	0.215
13	8.4	8.88	1.06	5.95	0.180
14	8.4	16.67	1.98	3.17	0.180
15	8.4	15.67	1.87	3.37	0.180
16	11.5	16.84	1.46	4.29	0.126
17	11.5	14.71	1.28	4.91	0.126
18	11.5	15.17	1.32	4.77	0.126
19	12.6	25.82	2.05	3.07	0.115
20	12.6	24.25	1.92	3.27	0.115
21	12.6	20.08	1.59	3.94	0.115

Table 4.2 Dimensionless wave numbers and Froude number at $S = 0.2\%$

Experiment Number	River layer height ($\tilde{H}$)/ cm	Average Wave length ($\tilde{L}$) / cm	Wave Length / River layer height	Non-Dimensional Wave number / k	River Froude Number / Fr
1	2.7	27.12	10.05	0.63	0.360
2	2.7	28.67	10.62	0.59	0.360
3	2.7	25.71	9.52	0.66	0.360
4	4.3	21.27	4.95	1.27	0.359
5	4.3	22.19	5.16	1.22	0.359
6	4.3	20.86	4.85	1.30	0.359
7	6.5	24.27	3.73	1.68	0.213
8	6.5	24.93	3.83	1.64	0.213
9	6.5	18.53	2.85	2.20	0.213
10	7.4	19.09	2.58	2.44	0.206
11	7.4	19.61	2.65	2.37	0.206
12	7.4	20.79	2.81	2.24	0.206
13	8	25.04	3.13	2.01	0.194

14	8	29.39	3.67	1.71	0.194
15	8	31.11	3.89	1.62	0.194
16	11.3	16.87	1.49	4.21	0.130
17	11.3	20.78	1.84	3.42	0.130
18	11.3	19.55	1.73	3.63	0.130

Average wave lengths are plotted against the river layer height and shown in Figure 4.9 and Figure 4.10. Also the same data are plotted in the one diagram in Figure 4.11. These three figures are for the dimensional values.

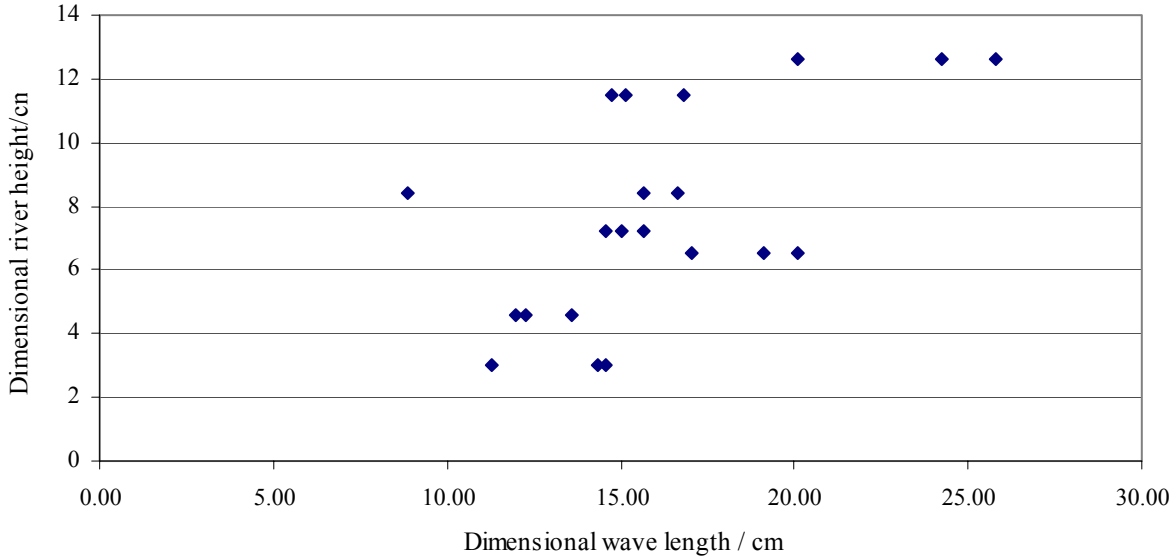

Figure 4.9 Dimensional river heights vs. Dimensional wave lengths for S=0.1%

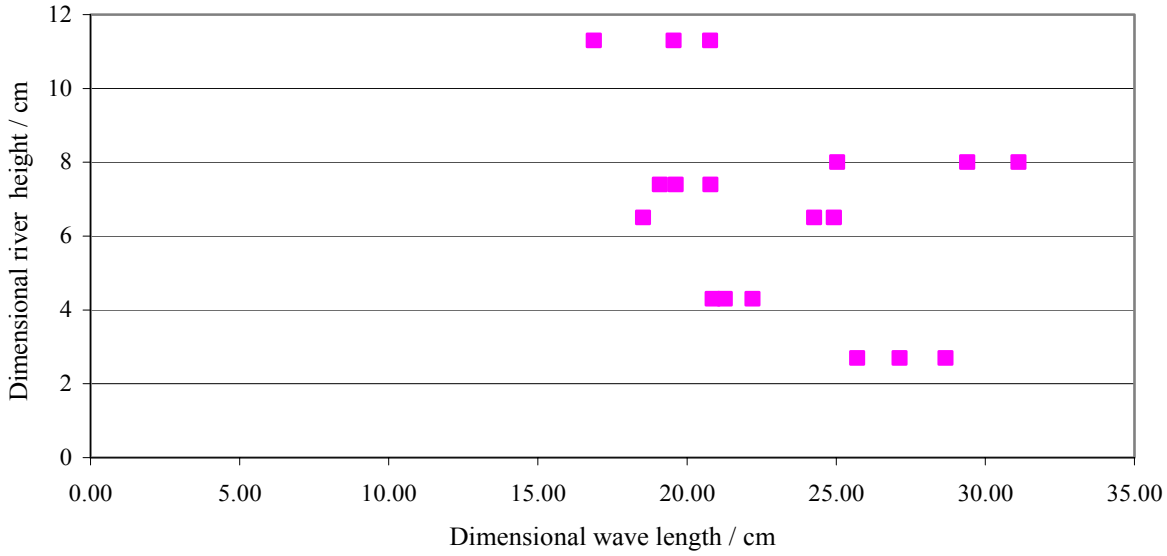

Figure 4.10 Dimensional river heights vs. Dimensional wave lengths for S=0.2%

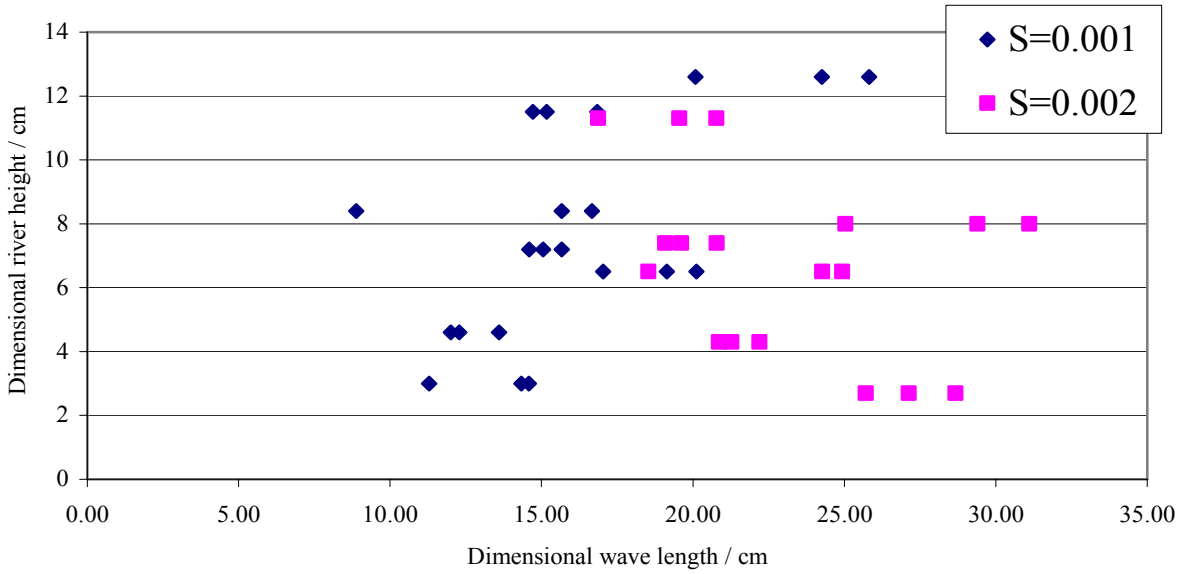

Figure 4.11 Dimensional river heights vs. Dimensional wave lengths for both slopes

The calculated Froude numbers are plotted against the dimensionless dominant wave number and shown in the Figure 4.12 and Figure 4.13. Also the same data are plotted in the one diagram in order to compare the data against the slope of the combined system in Figure 4.14.

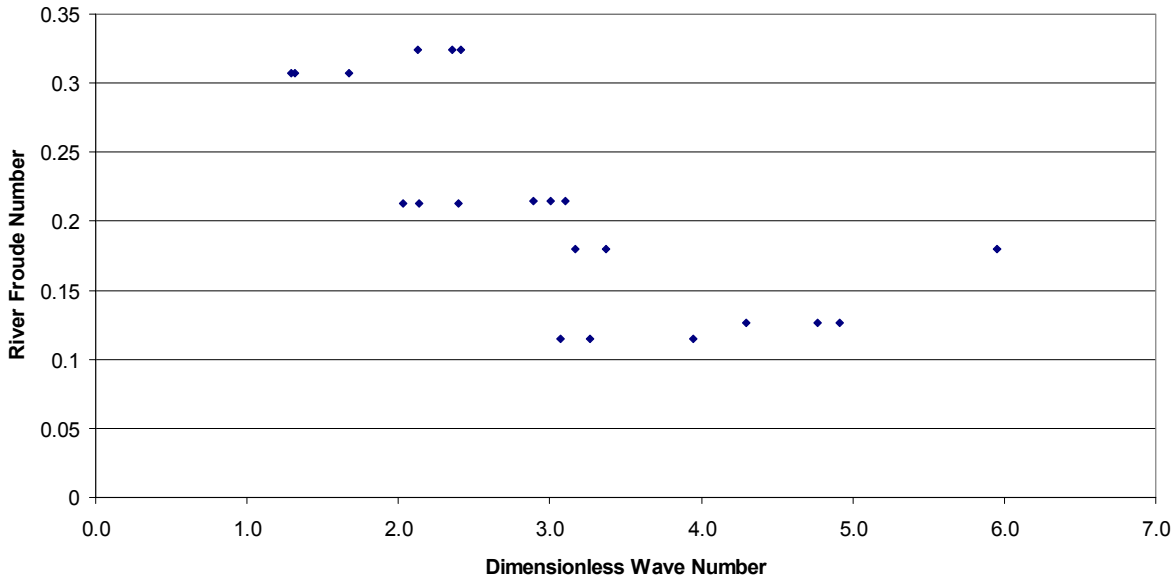

Figure 4.12 Froude numbers vs. Dimensionless Dominant Wave Numbers for S=0.1%

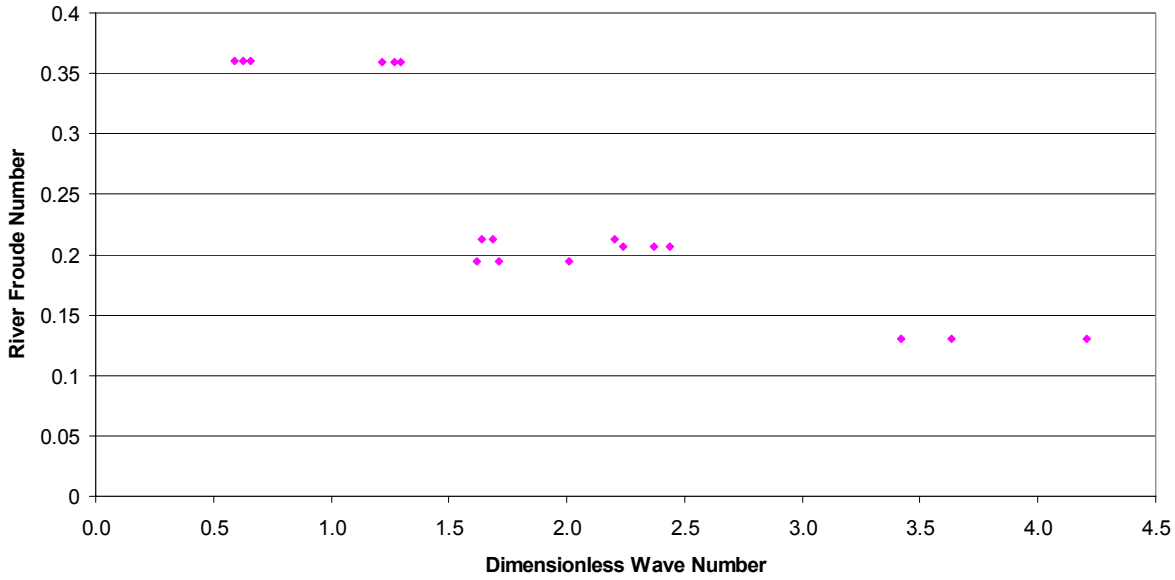

Figure 4.13 Froude Numbers vs. Dimensionless Dominant Wave Numbers for S=0.2%

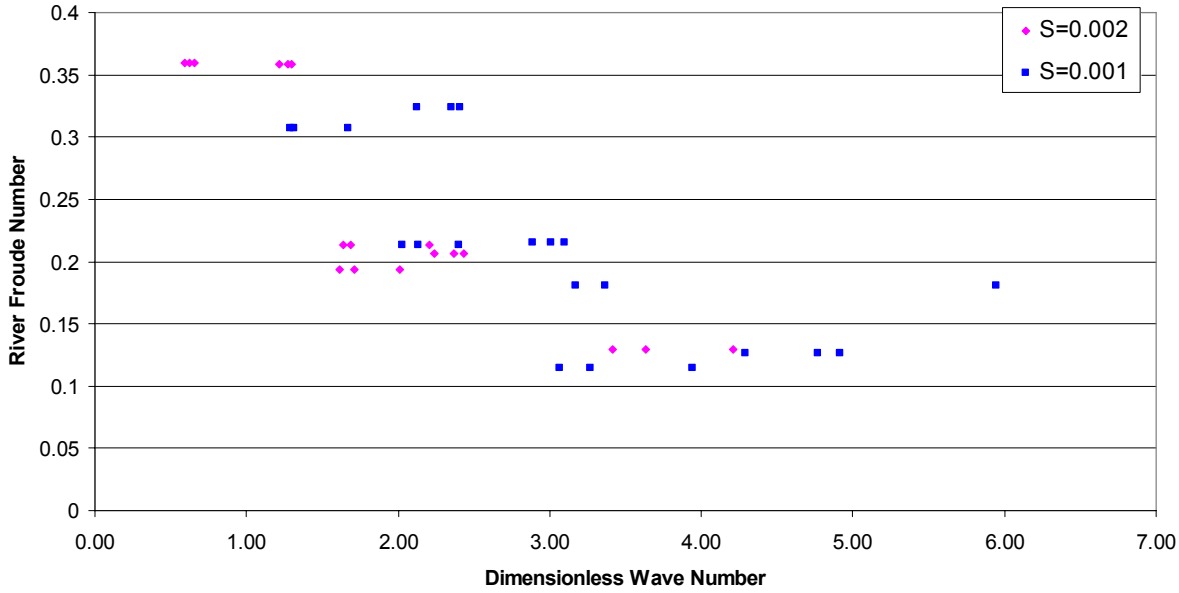

Figure 4.14 Froude Number vs. Dimensionless Dominant Wave Number for both slopes

4.6 CONCLUSIONS

From the observations it can be clearly visualized the river flow and seepage flow interactions. It cannot be clearly seen a definite combination or a relation between the river flow height and the wave lengths from the Figures 4.9 – 4.11. The dominant wave lengths are scattered in between 10 to 30 cm. However by examining Figures 4.12 and 4.13, it can be clearly understood a relationship between the Froude number of the river flow and the non-dimensional dominant wave numbers. This can be

concluded that the non-dimensional dominant wave numbers for the interactions are increased with the decrease of the Froude number of the river flow.

In addition, it can be seen that the dimensionless dominant wave numbers have an effect on the combined channel slope from the Figure 4.14. With the slope it can be concluded that the dimensionless dominant wave numbers are reached to the Froude number axis, or else the value of the dimensionless dominant wave numbers are decreased.

From the experiments there are some observational conclusions and author would like to present them at this stage. Quick river flow and seepage flow interactions are occurred, when the height of the river layer is comparably small with the Hele-Shaw model, whereas slow river flow and seepage flow interactions are occurred, when the height of the river layer is comparably large with the Hele-Shaw model. With this observation, it can be concluded that the residence time of hyporheic interactions are increased with the height of the river layer.

When the river layer height is less than or equal to the Hele-Shaw model height, wavy form of the hyporheic interactions are clearly visualized, whereas the wavy form of hyporheic interactions are not clearly visualized, when the river layer height is higher than the Hele-Shaw model height. At the second stage the author was able to see the sudden pop up of dye as shown in Figures 4.15 and 4.16.

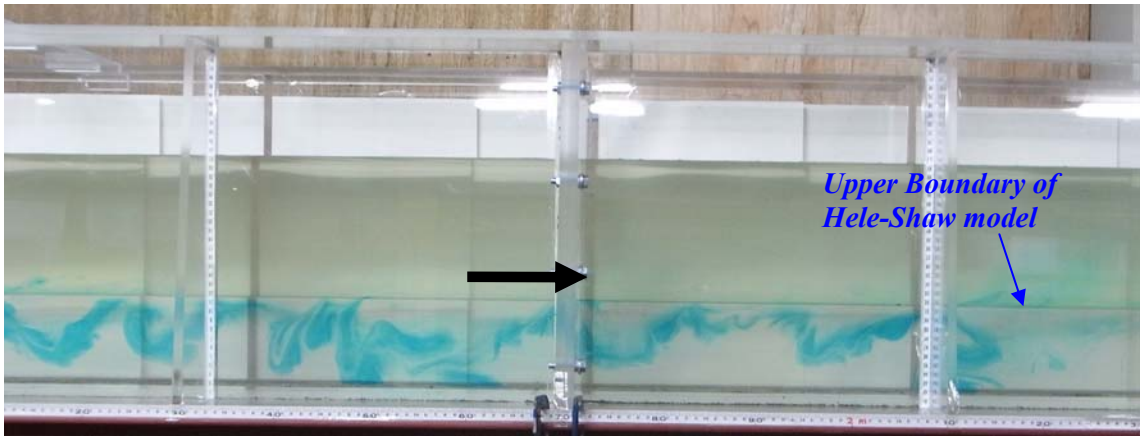

Figure 4.15 Interactions at 0.1% slope when the river height is 15.9 cm

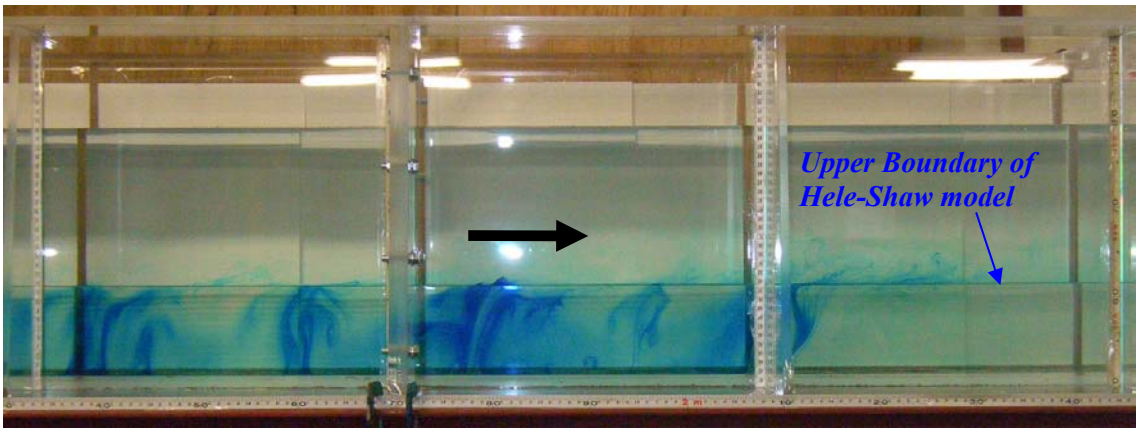

Figure 4.16 Interactions at 0.2% slope when the river height is 17.6 cm

Chapter 5

COMPARISON BETWEEN THEORETICAL ANALYSIS RESULTS AND THE EXPERIMENTAL OBSERVATIONS

5.1 INTRODUCTION

A rough comparison between the theoretical results and the experimental observations is carried out. In order to interpret the dimensionless particle diameter of the sediment in the seepage layer a rough assumption is used.

5.2 DIMENSIONLESS PARTICLE DIAMETER FOR THE EXPERIMENTS

Dimensionless particle diameter for the theoretical analysis is shown in the equation (5.1) as same as the equation (3.91).

$$D_P = \frac{\tilde{d}_P}{\tilde{H}_n} \tag{5.1}$$

where $\tilde{d}_P$ and $\tilde{H}_n$ are the dimensional particle diameter of the sediment and the uniform river flow height respectively. For the experiments as assumption is made as shown follows, in order to find the corresponding dimensional particle diameter.

$$\tilde{d}_P = \frac{d}{4} \tag{5.2}$$

where d is the thickness of the Hele-Shaw model plates.

Based on this assumption, dimensionless particle diameter for each and every case is calculated with the use of uniform river flow height.

5.3 THEORETICAL ANALYSIS WITH THE EXPERIMENTAL OBSERVATIONS

Dimensionless particle diameter is plotted against the dimensionless dominant wave numbers for the experiments as shown in Figures 5.1 and 5.2.

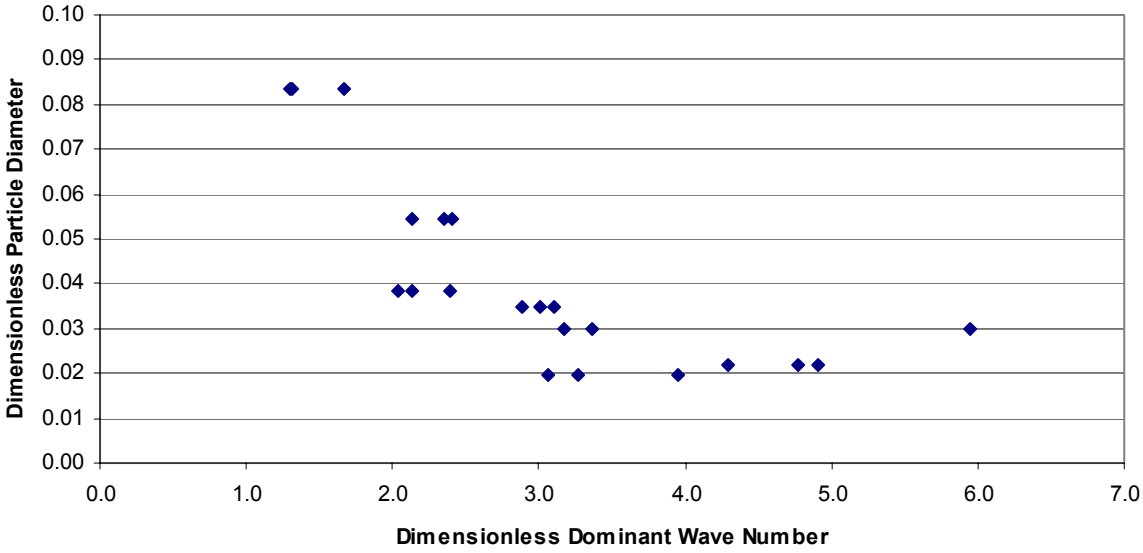

Figure 5.1 Dimensionless particle diameter vs. Dimensionless dominant wave numbers for S=0.1%

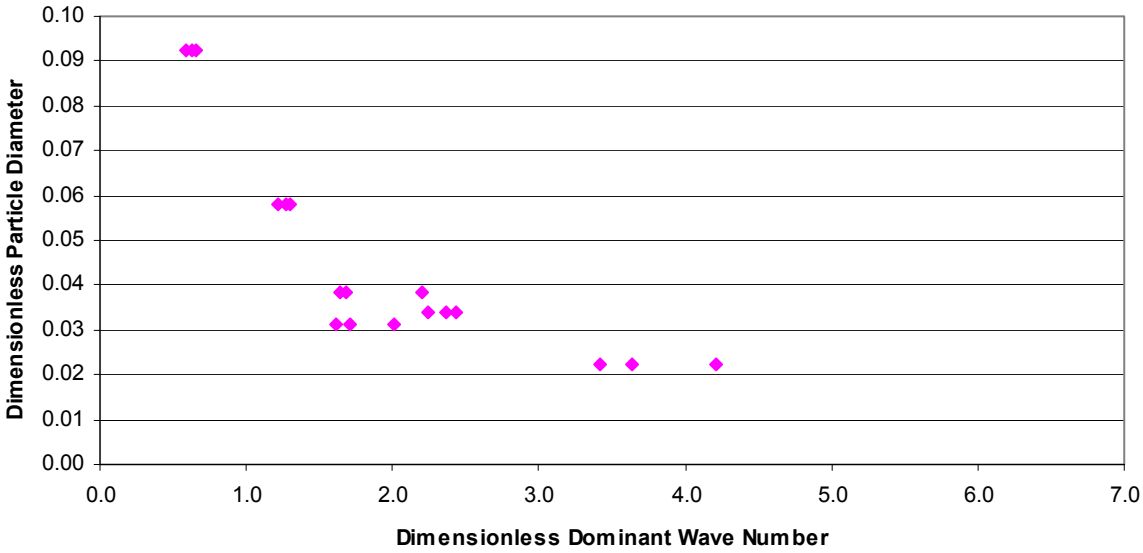

Figure 5.2 Dimensionless particle diameter vs. Dimensionless dominant wave numbers for S=0.2%

These calculated values for the experiments, in both slopes are plotted with the theoretical results in the same figures as shown in Figures 5.3 and 5.4.

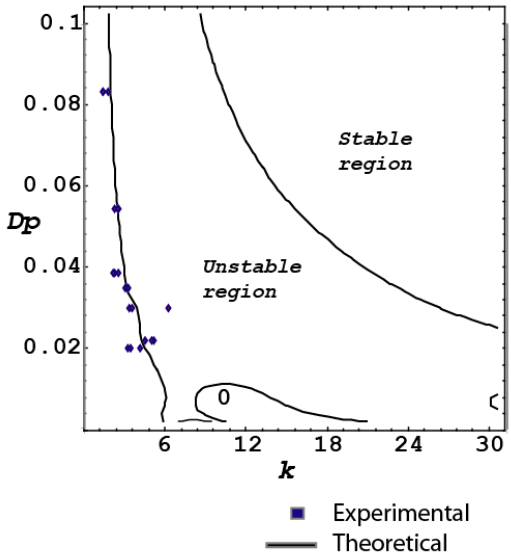

Figure 5.3 Theoretical analysis with the experimental observations for S=0.1%

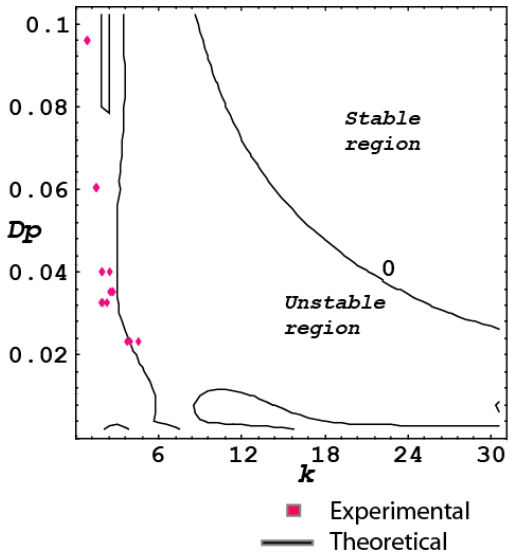

Figure 5.4 Theoretical analysis with the experimental observations for S=0.2%

5.4 CONCLUSIONS

Even though rough assumption is not perfect for the comparison, it can be clearly seen that the dimensionless dominant wave numbers which are obtained from the experiments are laid with the neutral curve of the theoretical contour maps in both 0.1% and 0.2% slopes. However these experimental dimensionless dominant wave numbers at interactions are smaller than the theoretical dimensionless wave numbers. This may be due to the non-linearity of the problem and the various disturbances in the experiments.

Chapter 6

RECOMMENDATIONS

For further research on this topic the author would like to suggest the following recommendations.

- Even though the theoretical model for the interactions between river flow and seepage flow is set from the Chapter 3, it is highly recommended to carry out an experimental investigation to verify the results with the sediments.

- Since the linear stability analysis is valid for the initiation of the interactions higher order analysis, like non-linear analysis is recommended.

- As discussed in Chapter 3, the stability analysis is carried out to the flat bed conditions of the river bed. However from the literature the author was found that the bed morphology has an advantageous effect on the river and seepage flow interactions. Therefore it is recommended to pursue the stability analysis for movable bed by including the governing equations of the sediment transport.

- Further experimental work with the Hele-Shaw model, using a lengthy channel is recommended.

- Theoretical analysis for the interactions between the channel flow and the Hele-Shaw flow should be carried out to understand the experimental observations.

APPENDIX

List of Abbreviations

A	Amplitude of small perturbation
b	Dimensional gap or space between two plates of the Hele-Shaw model
$\tilde{B}$	Width of the open channel
c_F	Non-Dimensional Forchheimer coefficient
d	Dimensional thickness of the plate of the Hele-Shaw model
$\tilde{d}_p$	Dimensional particle diameter of the bed material
D_P	Non-dimensional particle diameter of the bed material
e_{ns}	Unit vector in the direction normal to the water surface
e_{ts}	Unit vector in the direction tangential to the water surface
$\tilde{g}_i$	Gravitational acceleration component in "i" direction
h	Non-dimensional height of seepage flow
$\tilde{h}$	Dimensional height of seepage flow
H	Non-dimensional height of the river flow
$\tilde{H}$	Dimensional height of the river flow
$\tilde{H}_n$	Dimensional height of the river flow in normal flow condition
k	Non-dimensional wave number
K	Non-dimensional permeability of the seepage layer
$\tilde{K}$	Dimensional permeability of the seepage layer
l	Non-dimensional mixing length
$\tilde{p}$	Dimensional pressure in the seepage layer
P	Non-dimensional form of the pressure in river flow
$\tilde{P}$	Dimensional form of the pressure in river flow
$\tilde{Q}$	Dimensional form of the discharge in the open channel
R	Reference level at which the velocity vanishes in the logarithmic velocity distribution
Re	Reynolds number for the Hele-Shaw flow
S	Combined slope of the river and seepage flows
t	Non-dimensional time scale for river flow
$\tilde{t}$	Dimensional time scale for river flow
$\tilde{T}$	Non-dimensional time scale for seepage flow
T_{ij}	Non-dimensional Reynolds stress tensor for river flow
$\tilde{T}_{ij}$	Dimensional Reynolds stress tensor for river flow
$\bar{u}$	Non-dimensional uniform constant velocity in the stream-wise direction of the seepage layer
$\tilde{u}$	Dimensional virtual velocity in the seepage layer in stream-wise direction

$\overline{\tilde{u}_{avg}}$ Dimensional average seepage velocity in stream-wise direction

U Non-dimensional velocity of fluid particles in river flow in stream-wise direction

$\tilde{U}$ Dimensional velocity of fluid particles in river flow in stream-wise direction

$\overline{U_{avg}}$ Non-dimensional depth averaged velocity for the open channel flow

$\overline{\tilde{U}_{avg}}$ Dimensional depth averaged velocity for the open channel flow

U_B Non-dimensional velocity at the bed of the river layer $(y = 0)$ in stream-wise direction

$\tilde{U}_i$ Dimensional velocity of fluid particles in river flow

$\tilde{U}_{fn}$ Dimensional shear velocity at normal flow

$\tilde{U}_r$ Typical dimensional velocity to non-dimensionalization of seepage velocity

$\tilde{v}$ Dimensional virtual velocity in the seepage layer in normal direction to stream-wise direction

$\tilde{v}_i$ Dimensional filtration velocity in the seepage layer

$\tilde{V}$ Dimensional velocity of fluid particles in river in normal direction to stream-wise direction

$\tilde{w}$ Dimensional velocity in Hele-Shaw model in $\tilde{z}$ direction

x Non-dimensional stream-wise direction

$\tilde{x}$ Dimensional stream-wise direction

$\tilde{y}$ Non-dimensional normal direction to the stream-wise direction

$\tilde{y}$ Dimensional normal direction to the stream-wise direction

$\tilde{z}$ Dimensional normal direction to both stream-wise direction and $\tilde{y}$ direction

θ Slope angle for both river and seepage flows

κ Karman constant

λ Porosity of the seepage layer

λ_0 Linear growth rate

λ_1 Landau constant

μ Non-dimensional dynamic viscosity of water

$\tilde{\mu}$ Dimensional dynamic viscosity of water

$\tilde{\mu}_e$ Dimensional form of the effective viscosity

$\tilde{\nu}$ Dimensional kinematics viscosity

ν_T Non-dimensional eddy viscosity

$\tilde{\nu}_T$ Dimensional eddy viscosity

$\tilde{\rho}$ Dimensional density of water in river

$\tilde{\tau}_{ij}$ Dimensional stress tensor for seepage flow

ω Complex angular frequency of the perturbation

View publication stats